Selective Dye Sorption and Metal Ions Sensing Behaviours of a New Cd-based MOF

Priyanka Manna,[a] Avantika Hasija,[b] Deepak Chopra[b] and Partha Mahata[a*]

[a]Department of Chemistry, Jadavpur University, Kolkata-700032, India. Email: parthachem@gmail.com

[b]Crystallography and Crystal Chemistry Laboratory, Department of Chemistry, Indian Institute of Science Education and Research Bhopal, Bhopal By-Pass Road, Bhopal, MP 462066, India

ELECTRONIC SUPPLEMENTARY INFORMATION

*Corresponding Authors, E-mail: parthachem@gmail.com

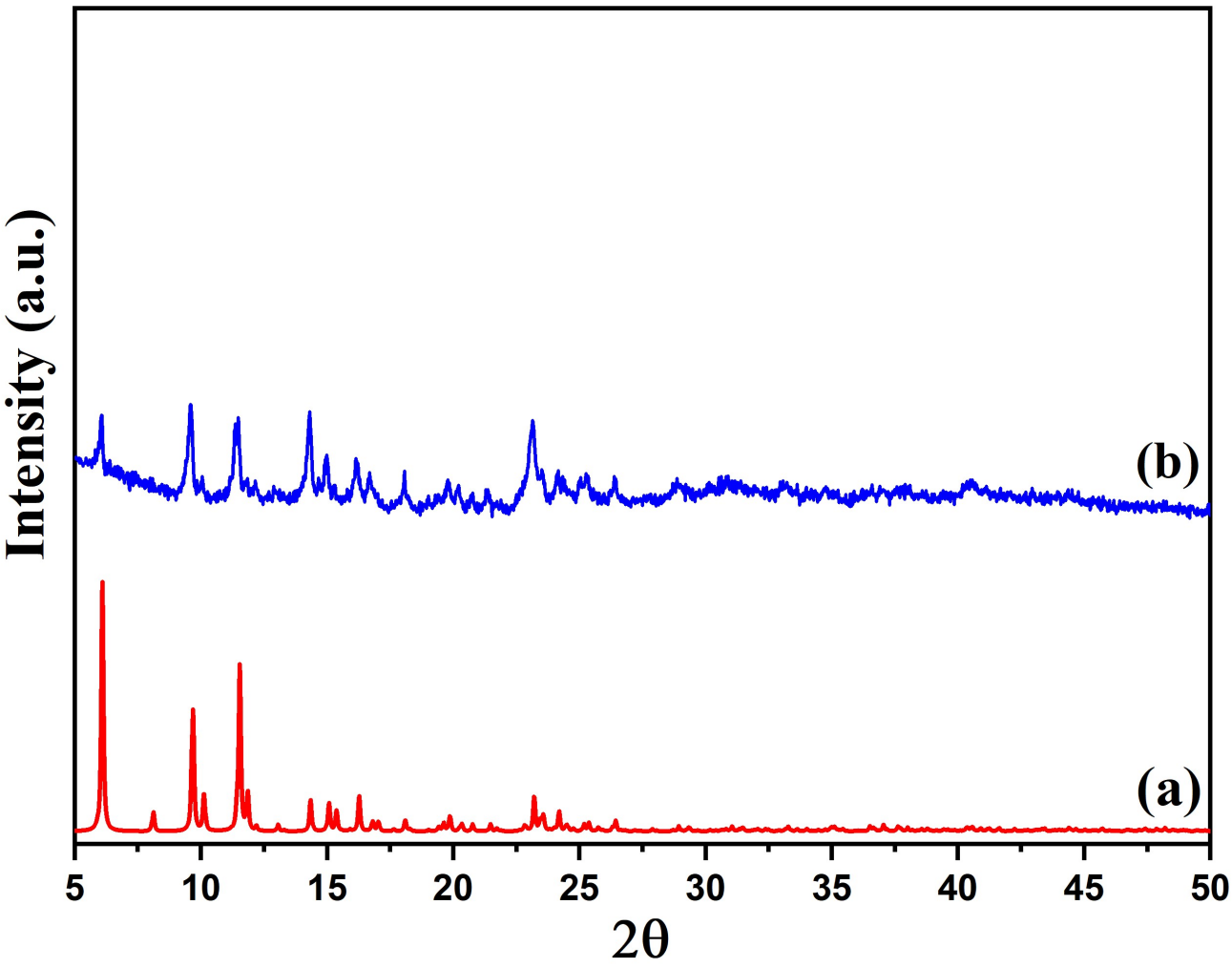

Fig. S1: Powder XRD (CuKα) patterns of [Cd(PDA)$(L)_2$], **1**: (a) simulated from single crystal X-ray data, (b) experimental.

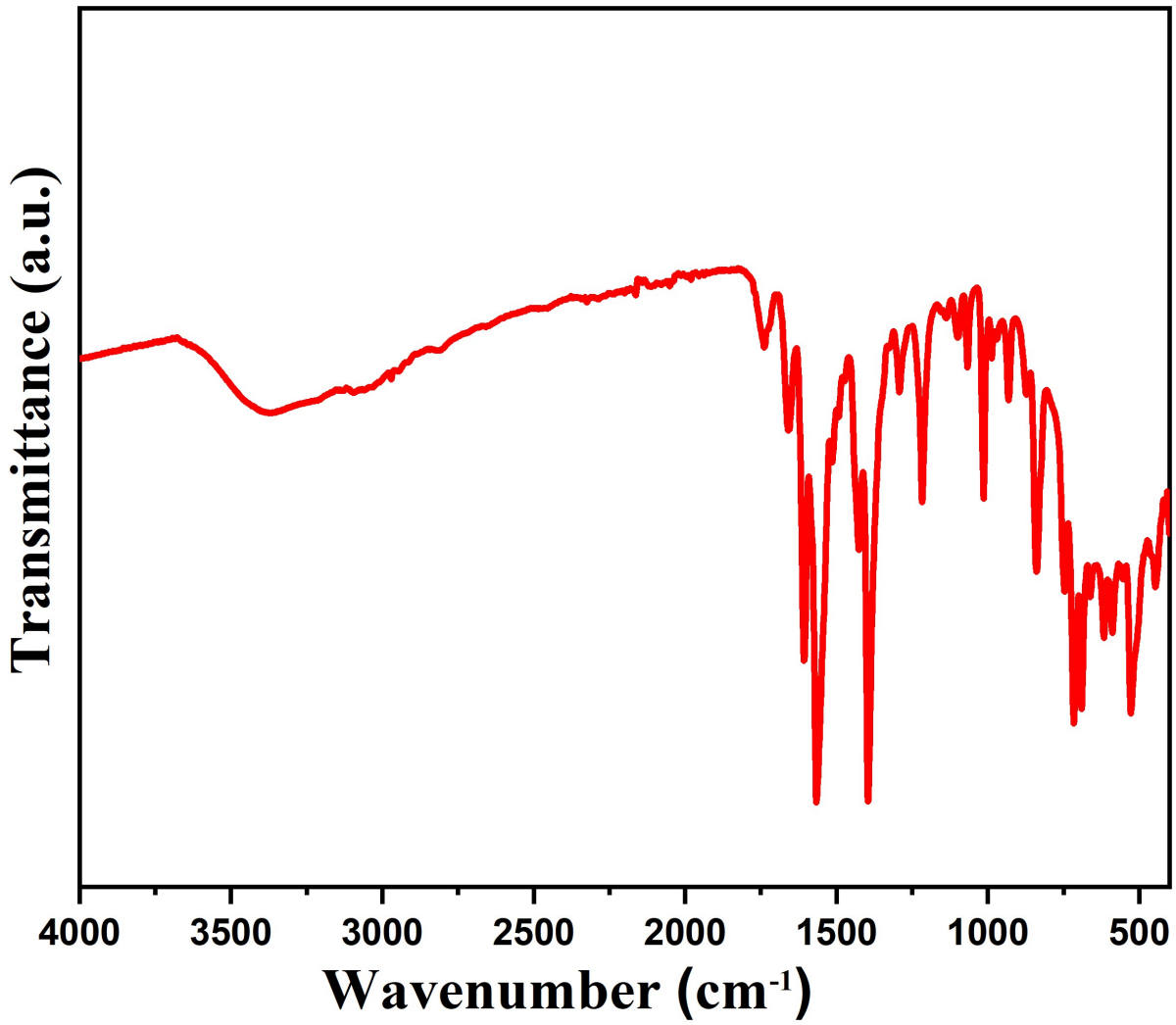

Fig. S2: IR spectrum of $[Cd(PDA)(L)_2]$, **1**.

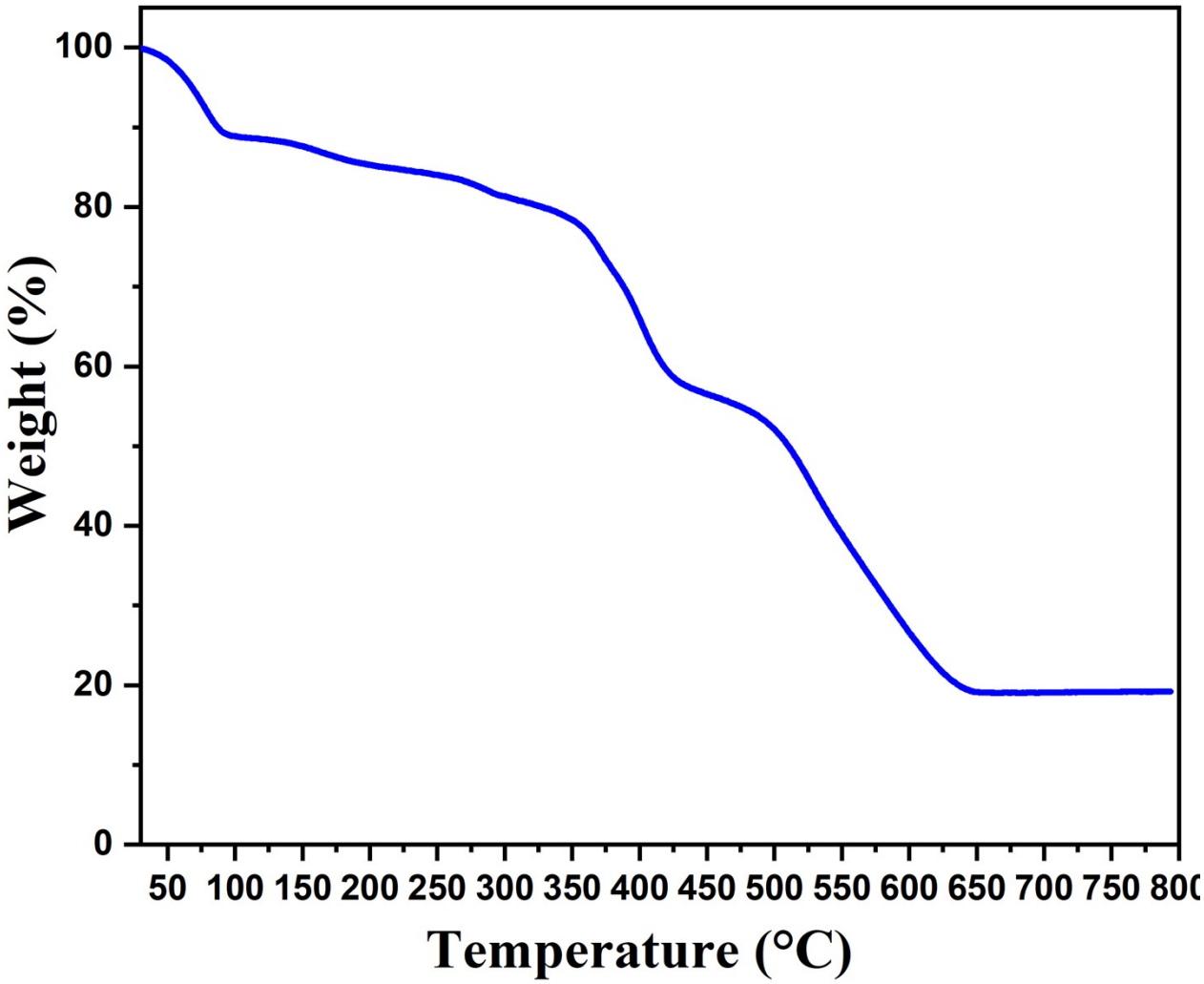

Fig. S3: Thermogravimetric analysis (TGA) of [Cd(PDA)$(L)_2$], **1**, in nitrogen atmosphere.

Table S1: Selected Bond Angles (deg) observed in [Cd(PDA)$(L)_2$], **1**.

Angle	Amplitude (º)
O (1) −Cd(1)−O(1) # 1	83.9 (3)
O (1) −Cd(1)−N(3) # 2	91.35 (17)
O (1) # 1 −Cd(1)−N(3) # 2	91.36 (17)
O (1) −Cd(1)−N(1)	91.57 (16)
O (1) # 1−Cd(1)−N(1)	91.57 (16)
N (3) # 2−Cd(1)−N(1)	176.1 (2)
O (1) −Cd(1)−N(2)	137.93 (13)
O (1) # 1−Cd(1)−N(2)	137.93 (13)
N (3) # 2−Cd(1)−N(2)	91.3 (3)
N (1) −Cd(1)−N(2)	84.7 (2)
O (1) −Cd(1)−O(2)	53.85 (17)
O (1) # 1−Cd(1)−O(2)	137.72 (18)
N (3) # 2−Cd(1)−O(2)	91.91 (13)
N (1) −Cd(1)−O(2)	87.70 (13)
N (2) −Cd(1)−O(2)	84.10 (11)
O (1) −Cd(1)−O(2) # 1	137.72 (17)
O (1) # 1 −Cd(1)−O(2) # 1	53.85 (17)
N (3) # 2 −Cd(1)−O(2) # 1	91.91 (13)
N (1) −Cd(1)−O(2)	87.70 (13)
N (2) −Cd(1)−O(2)	84.10 (11)
O (1) −Cd(1)−O(2) # 1	137.72 (17)
O (1) # 1 −Cd(1)−O(2) # 1	53.85 (17)
N (3) # 2 −Cd(1)−O(2) # 1	91.91 (13)
N (1) −Cd(1)−O(2) # 1	87.70 (13)
N (2) −Cd(1)−O(2) # 1	84.10 (12)
O (2) −Cd(1)−O(2) # 1	167.7 (2)

Symmetry transformations used to generate equivalent atoms:

For **1**: #1 -x+1, y, z; #2 -x+1, -y+1, -z+1.

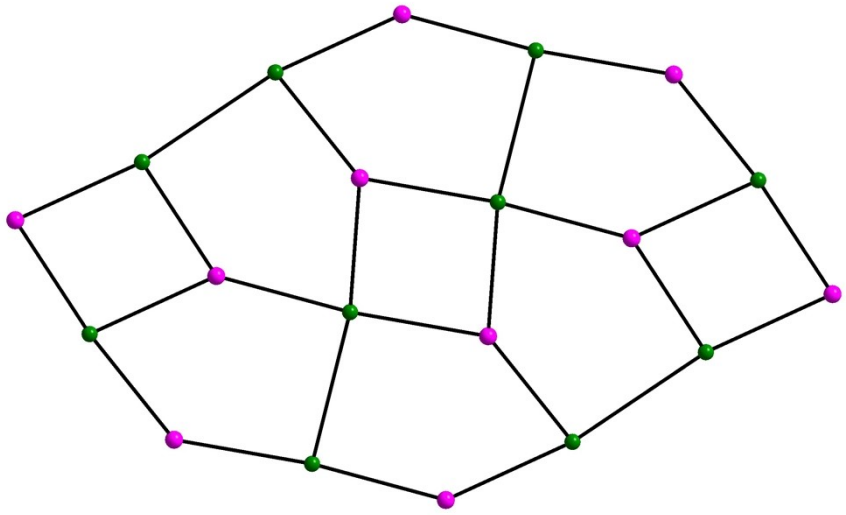

Fig. S4: Figure shows the network structure based on 3-connected L ligands and four connected Cd^{2+} ions of $[Cd(PDA)(L)_2]$, **1**.

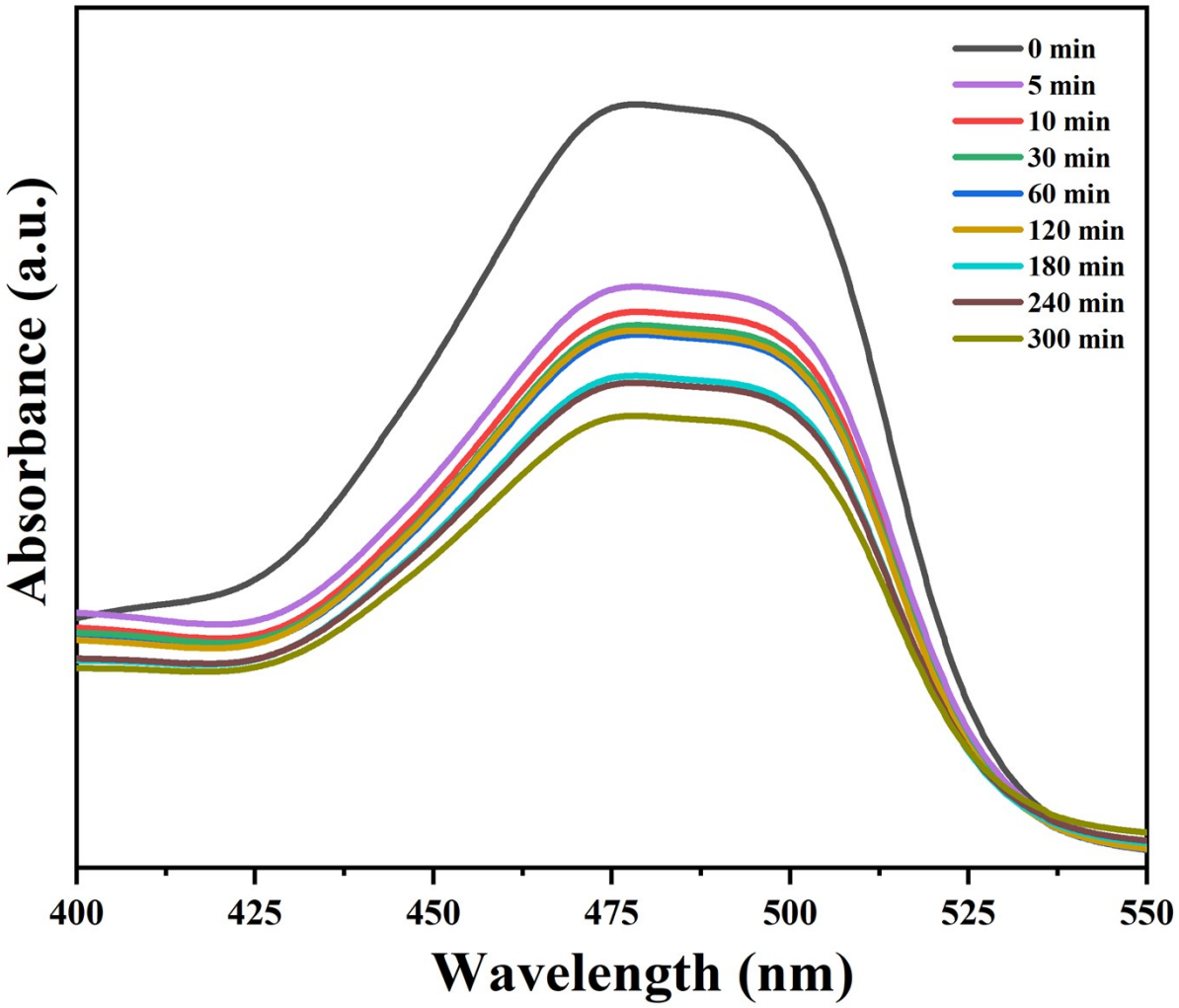

Fig. S5: UV-Vis absorption spectra of Orange G (OG) during the time dependent sorption study using compound **1**.

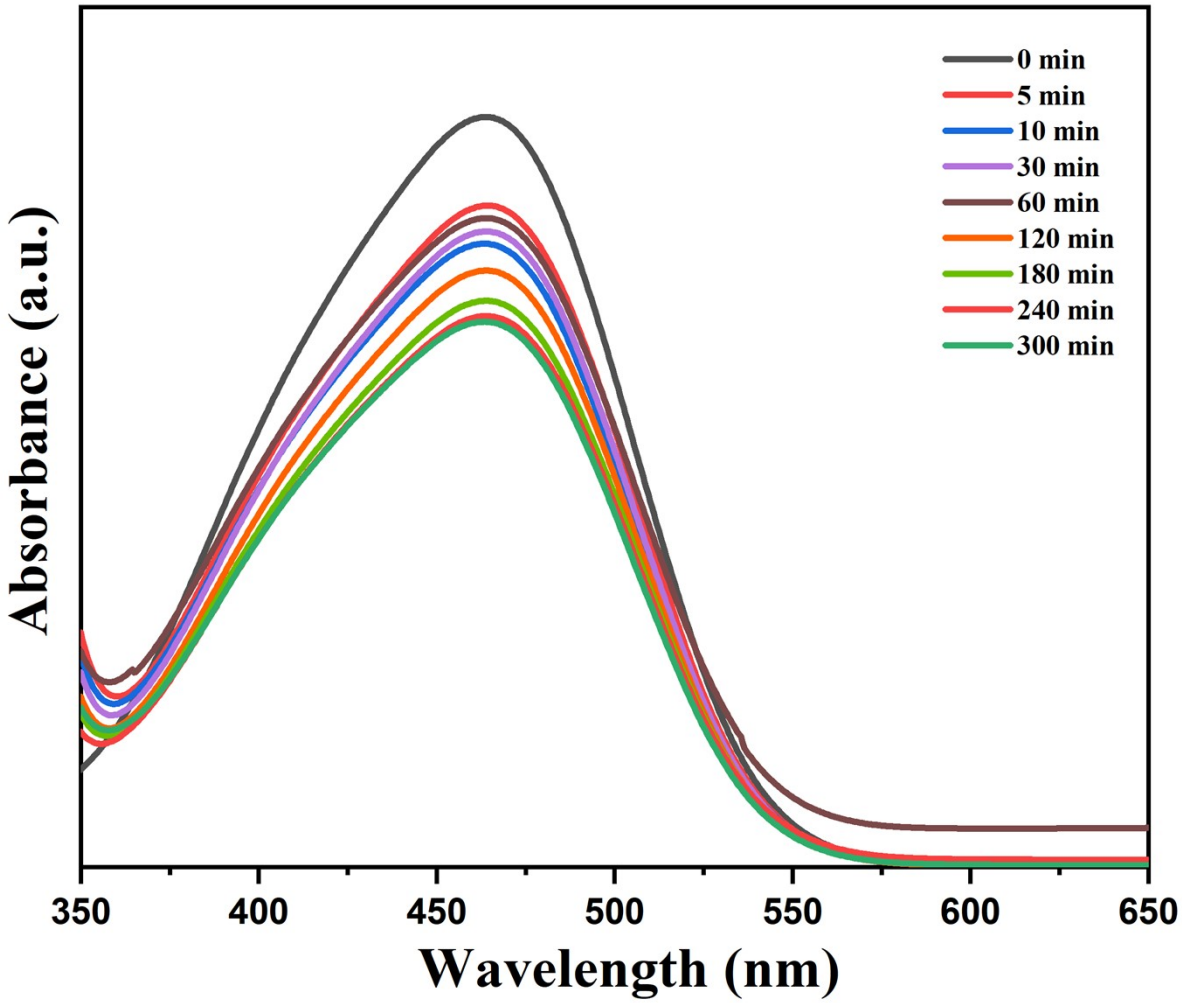

Fig. S6: UV-Vis absorption spectra of Methyl Orange (MO) during the time dependent sorption study using compound **1**.

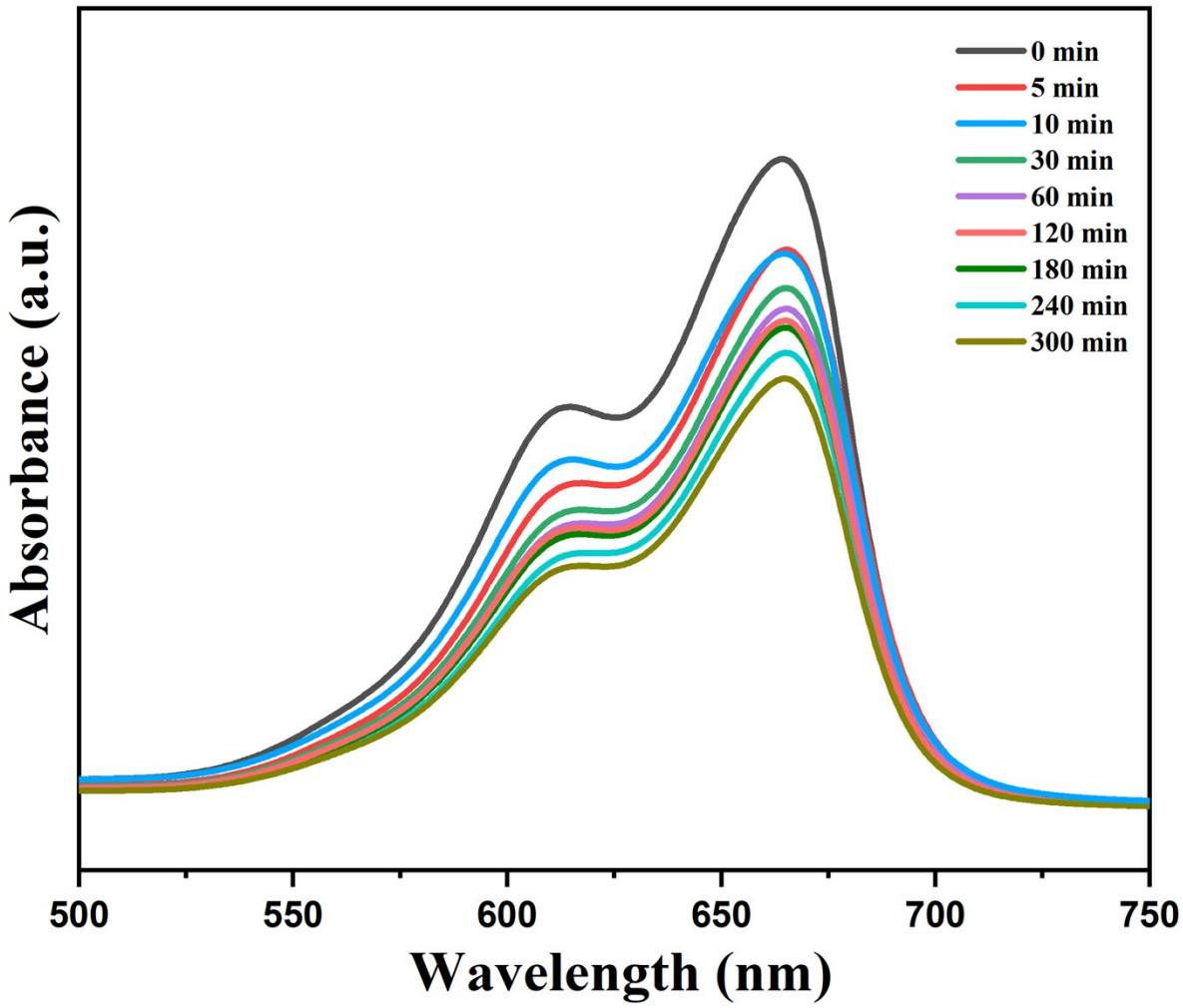

Fig. S7: UV-Vis absorption spectra of Methylene Blue (MB) during the time dependent sorption study using compound **1**.

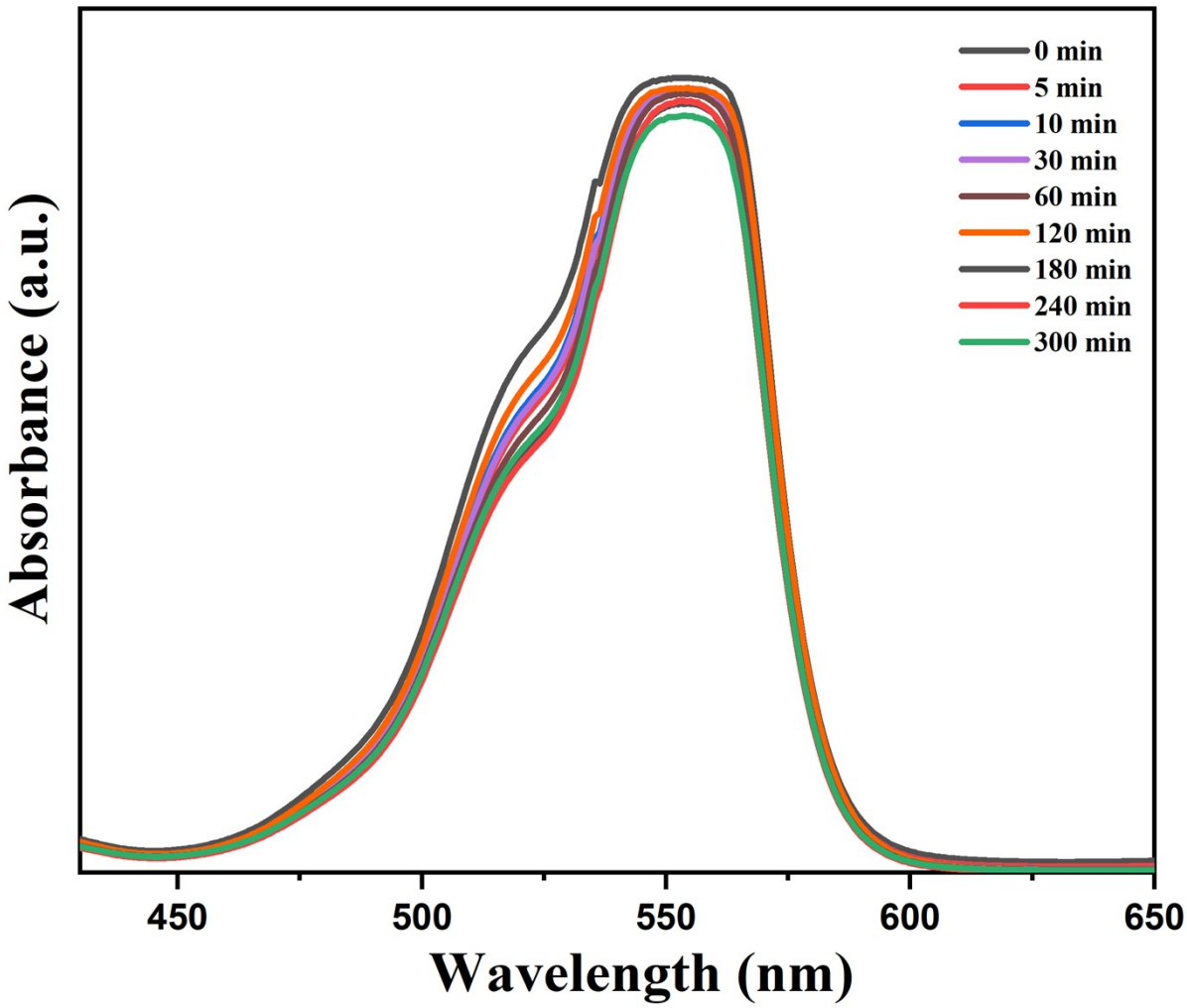

Fig. S8: UV-Vis absorption spectra of Rhodamine B (RhB) during the time dependent sorption study using compound **1**.

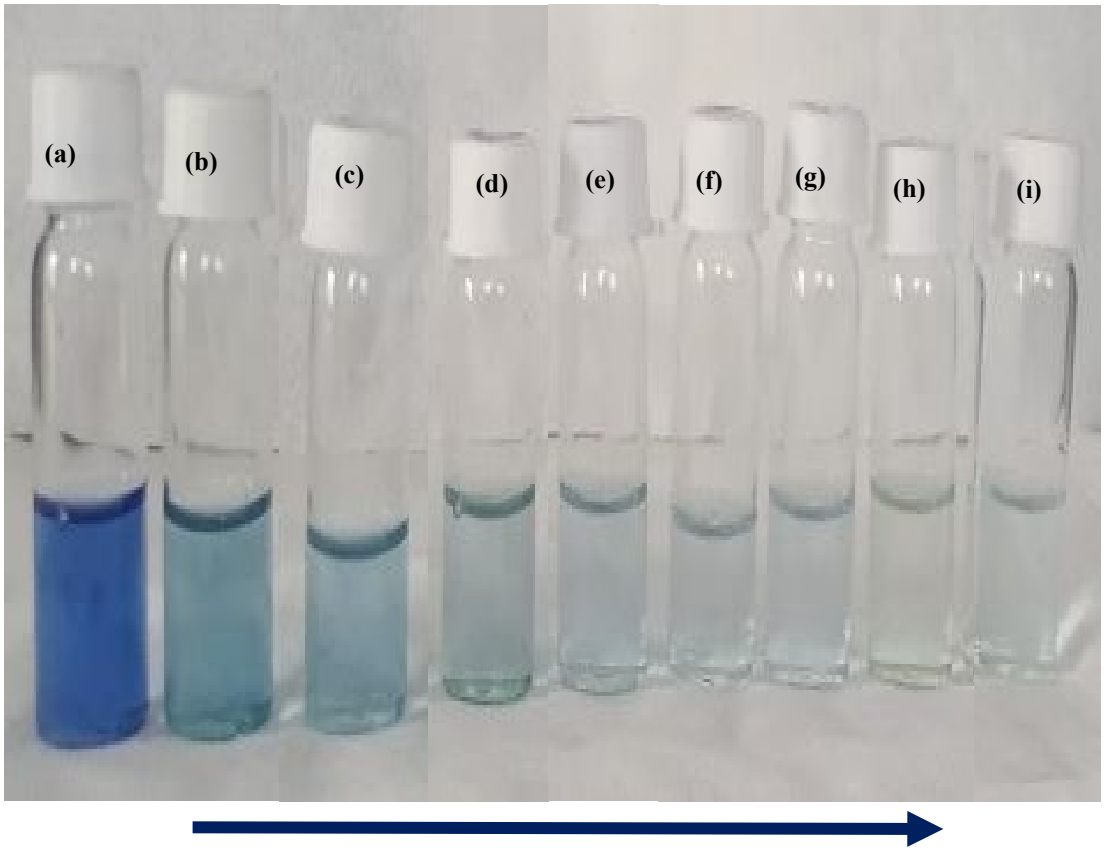

Fig. S9: Figure shows the photographs of colour intensity changes of the RBBR during the sorption study: (a) initial solution, (b) after 5 min, (c) after 10 min, (d) after 30 min, (e) after 60 min, (f) after 120 min, (h) after 180 min, (h) after 240 min, (i) after 300 min.

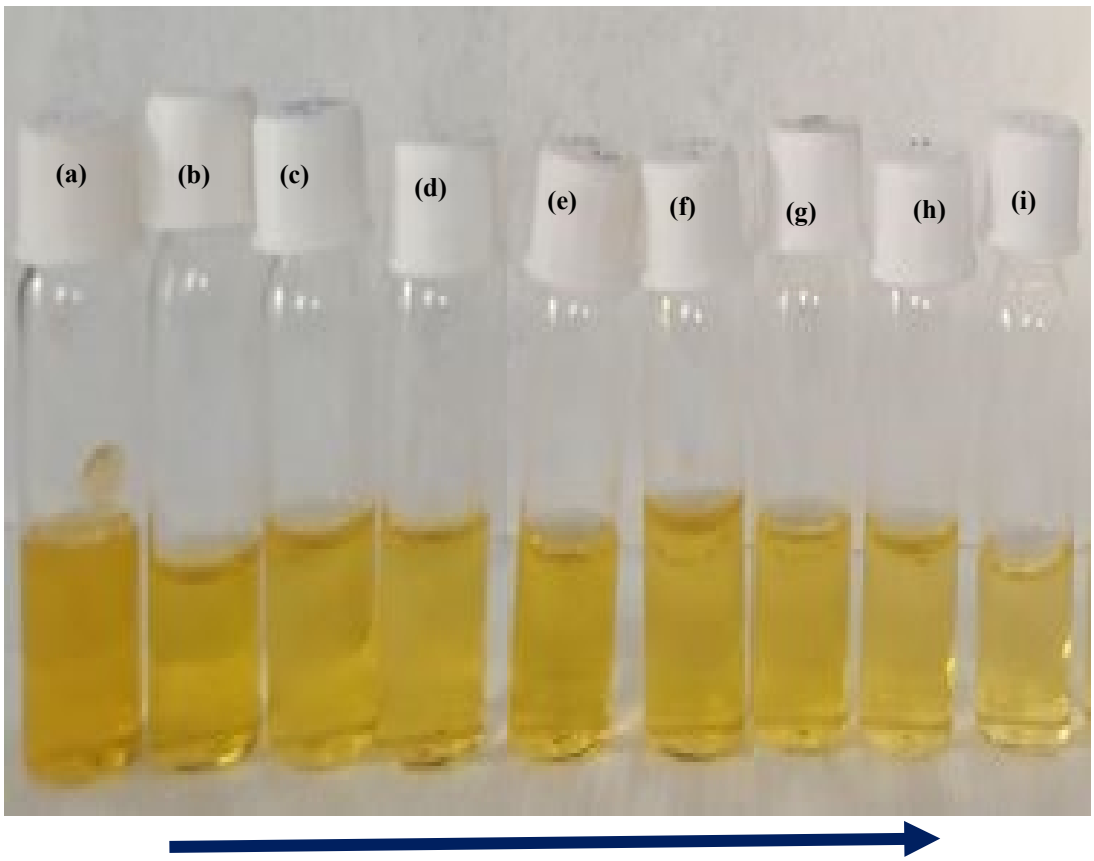

Fig. S10: Figure shows the photographs of colour intensity changes of the OG during the sorption study: (a) initial solution, (b) after 5 min, (c) after 10 min, (d) after 30 min, (e) after 60 min, (f) after 120 min, (h) after 180 min, (h) after 240 min, (i) after 300 min.

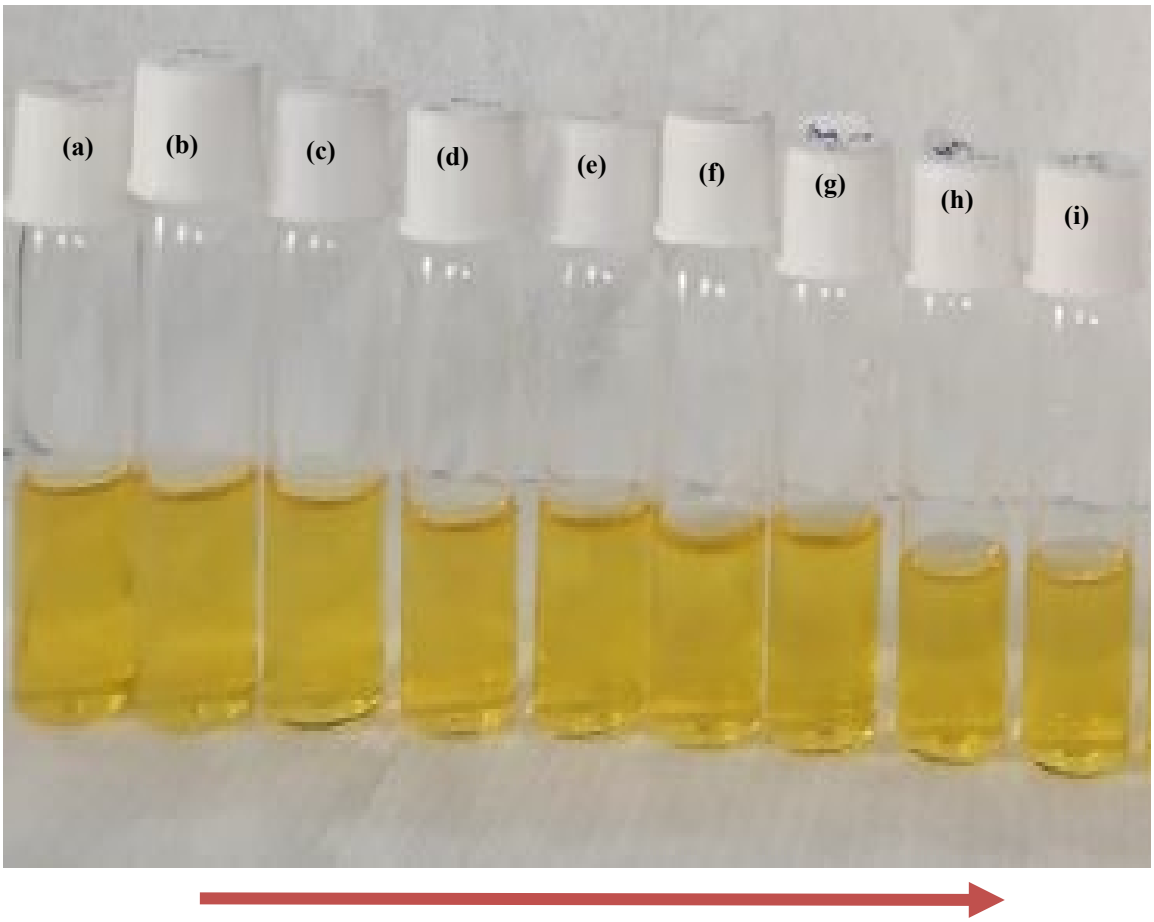

Fig. S11: Figure shows the photographs of colour intensity changes of the MO during the sorption study: (a) initial solution, (b) after 5 min, (c) after 10 min, (d) after 30 min, (e) after 60 min, (f) after 120 min, (h) after 180 min, (h) after 240 min, (i) after 300 min.

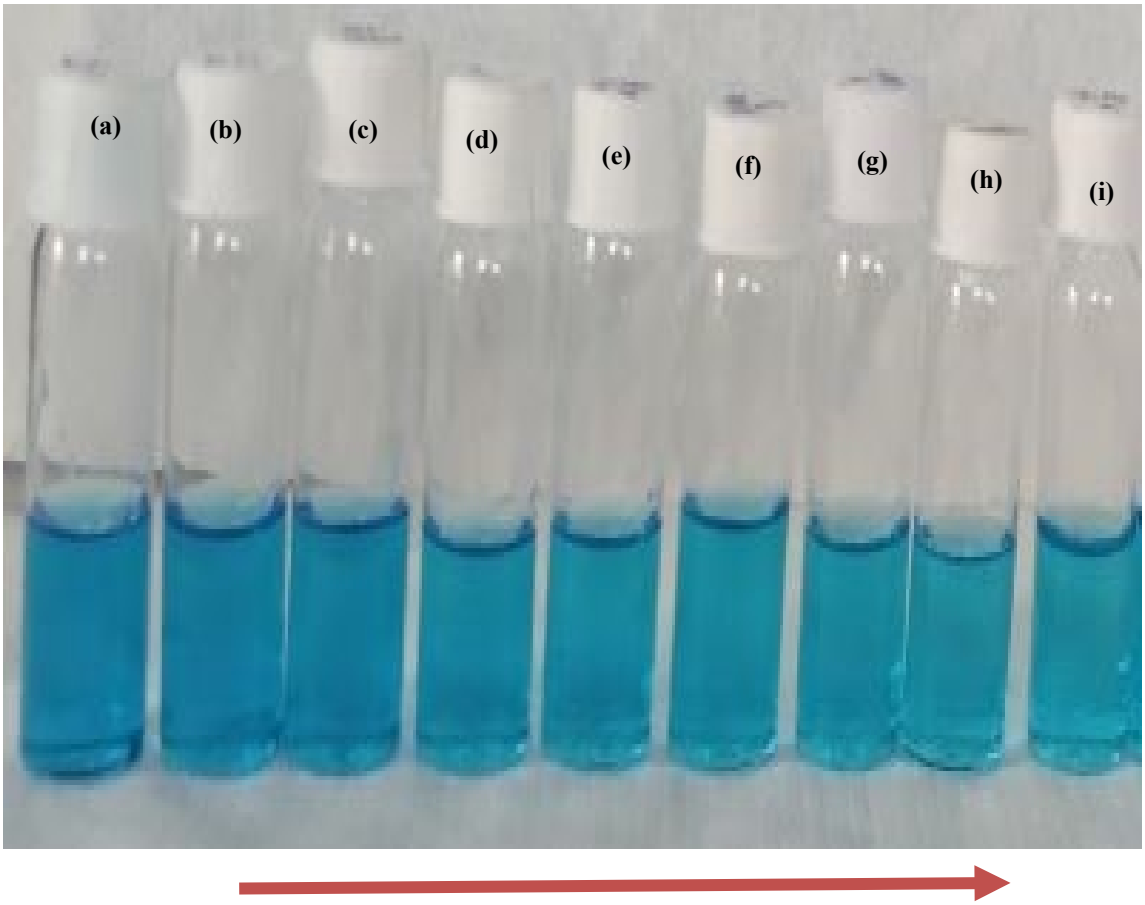

Fig. S12: Figure shows the photographs of colour intensity changes of the MB during the sorption study: (a) initial solution, (b) after 5 min, (c) after 10 min, (d) after 30 min, (e) after 60 min, (f) after 120 min, (h) after 180 min, (h) after 240 min, (i) after 300 min.

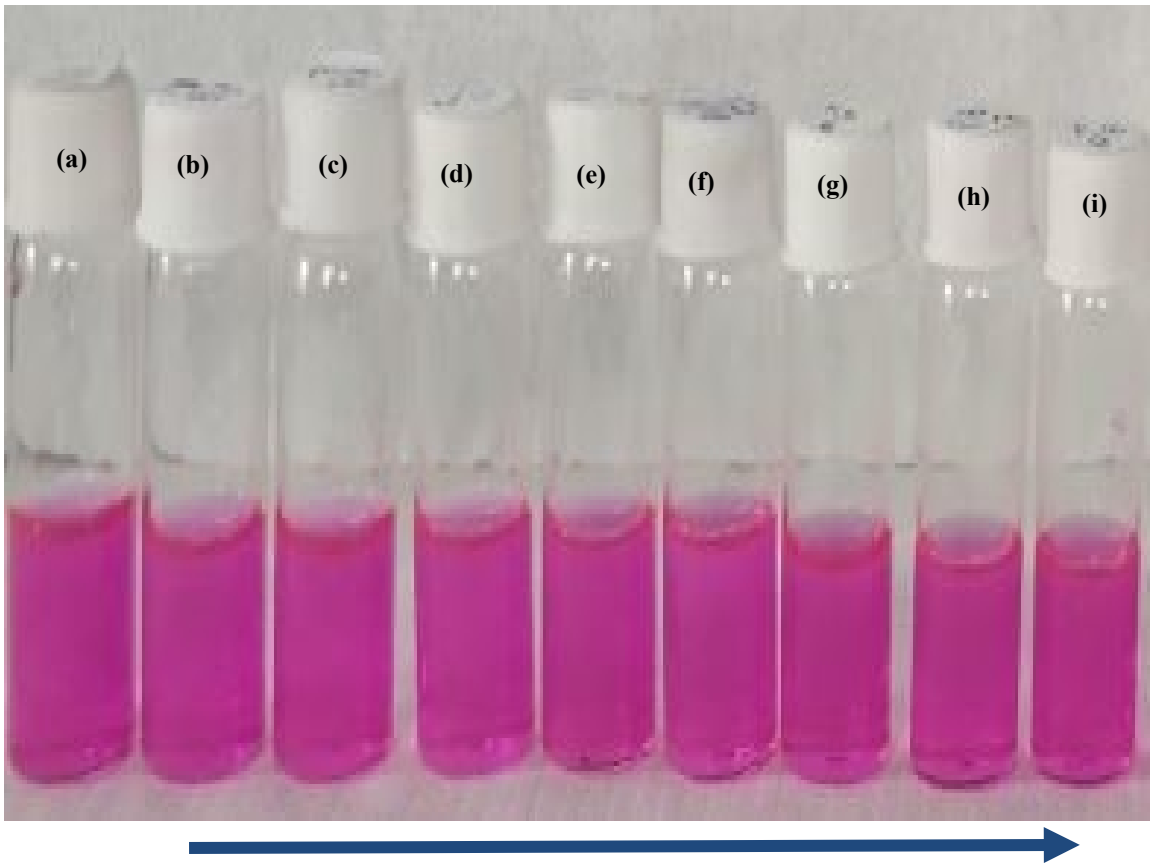

Fig. S13: Figure shows the photographs of colour intensity changes of the RhB during the sorption study: (a) initial solution, (b) after 5 min, (c) after 10 min, (d) after 30 min, (e) after 60 min, (f) after 120 min, (h) after 180 min, (h) after 240 min, (i) after 300 min.

Table S2: Pseudo-second-order kinetic parameters for RBBR dye sorption into $[Cd(PDA)(L)_2]$, 1.

Adsorbent	q_e(mg g^{-1})	K_2 (h g mg^{-1})	R^2
Cd-MOF	31.23	0.292	0.998
	61.50	0.112	0.996
	93.63	0.051	0.995
	123.15	0.056	0.997
	152.20	0.042	0.997

Table S3: Parameters of Langmuir model for RBBR dye sorption into [Cd(PDA)$(L)_2$], **1**.

Adsorbent	Dye	K_L (L mg^{-1})	Q_m (mg g^{-1})	R^2
Cd-MOF	RBBR	0.071	263.15	1

Table S4: A Summary of RBBR dye sorption using various materials.

Materials	Efficiency (%)	Time	Ref.
NMIL88(Fe)-Lac and HS NMIL88(Fe)-Lac	90.8 and 92.0	3 h and 2 h	79
ZIF-8 and ZIF-67	98 and 95	2 h	80
TiO_2-ZrO_2- Laccase and TiO_2-ZrO_2-SiO_2- Laccase	90 and 76	24 h	81
Magnetic copper alginate beads	75.8	4 h	82
CS-SA/ALG/MTN	54.3	½ h	83
Immobilized laccase	64	48 h	84
PU microspheres	64.1	6 h	85
Trametes maxima IIPLC-32	92.3	—	86
Amberlyst A21	89.23	2½ h	87
Thuja orientalis (ACTOL)	82	5 h	88
$[Cd(PDA)(L)_2]$	95	5 h	This work

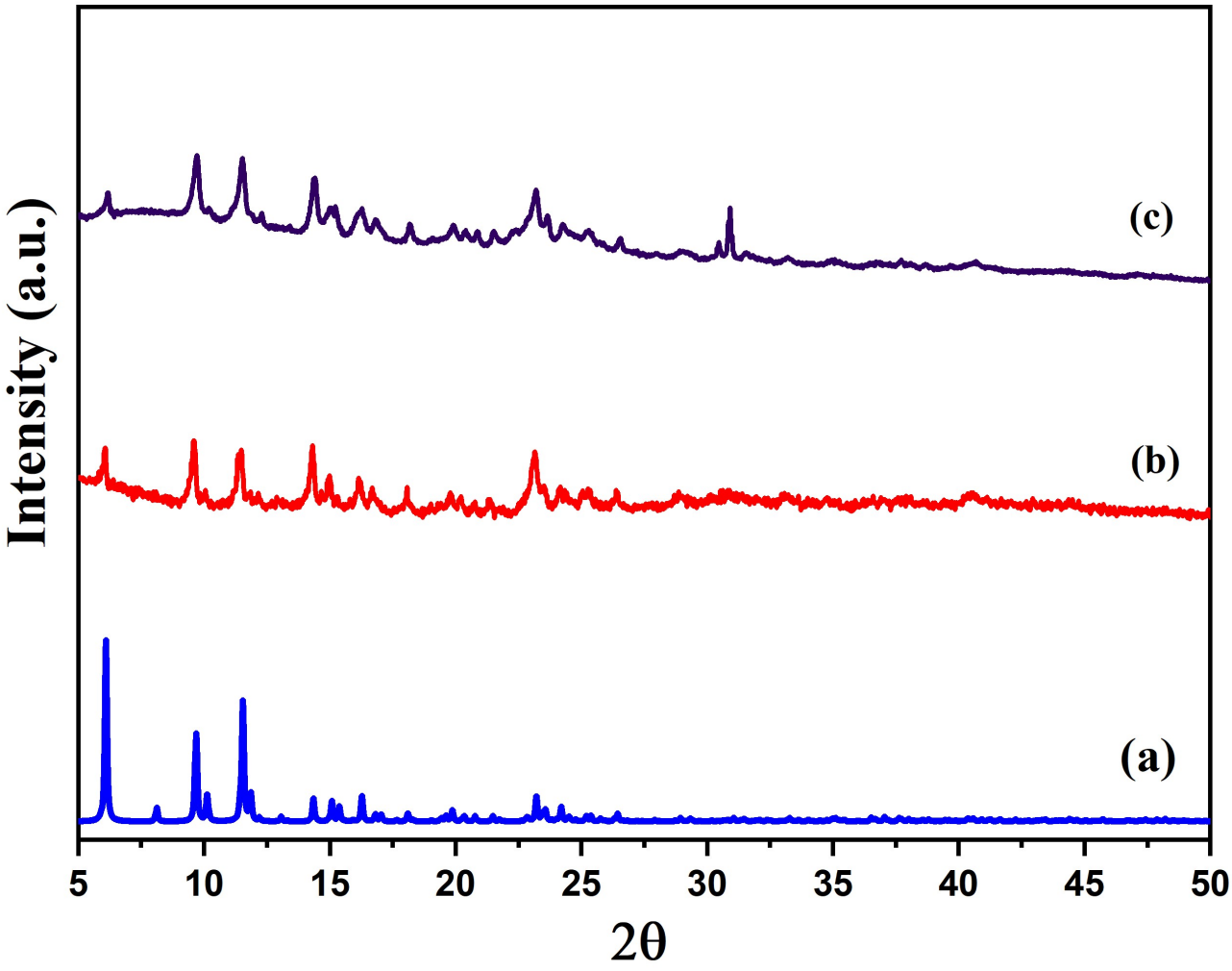

Fig. S14: Powder XRD (CuKα) patterns of [Cd(PDA)$(L)_2$], **1**: (a) simulated from single crystal X-ray data, (b) experimental. (c) RBBR@**1** after 300 min.

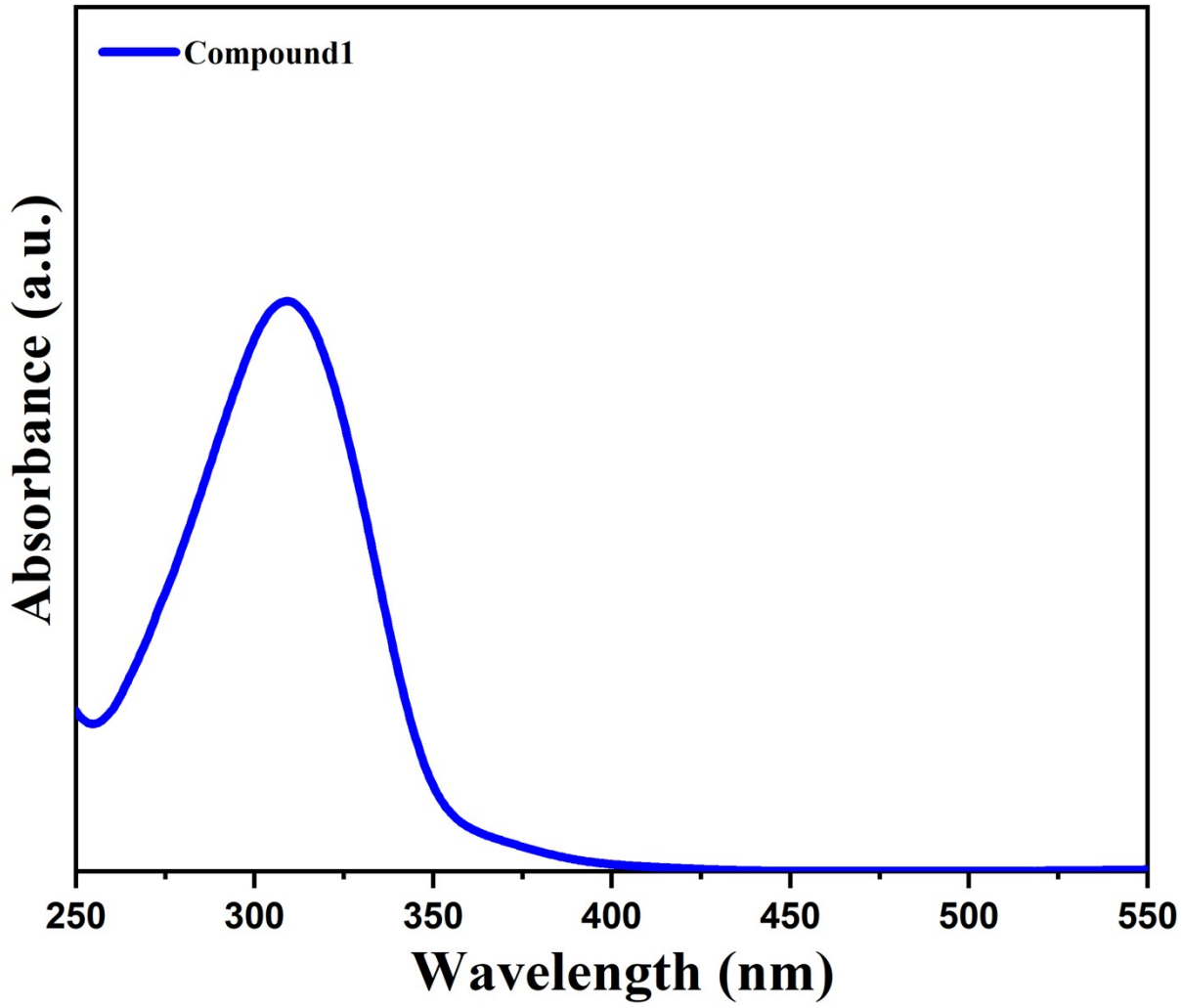

Fig. S15: Absorption spectrum of [Cd(PDA)$(L)_2$], **1**.

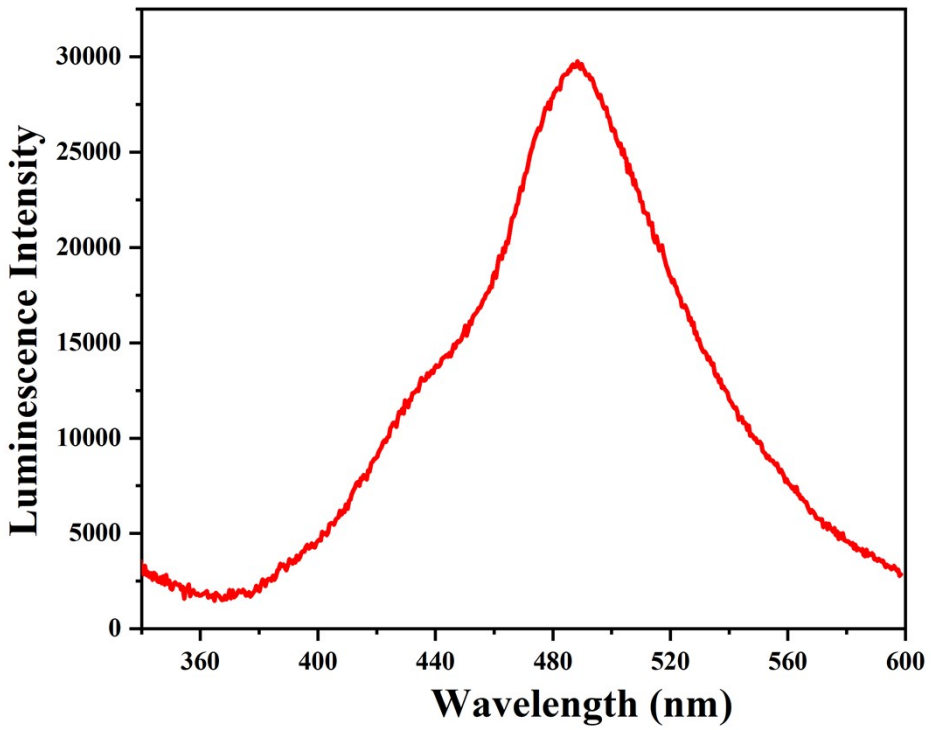

Fig. S16: Emission spectra of **1** in solid state (λ_{ex} = 300 nm).

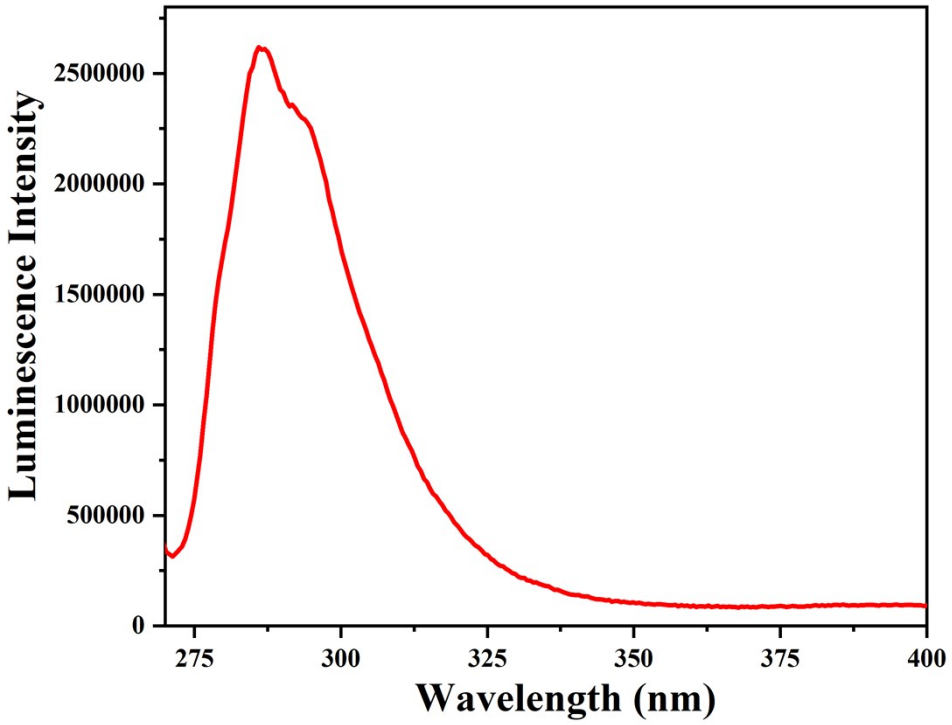

Fig. S17: Emission spectra of 1,4-phenylenediacetic acid in solid state (λ_{ex} = 263 nm).

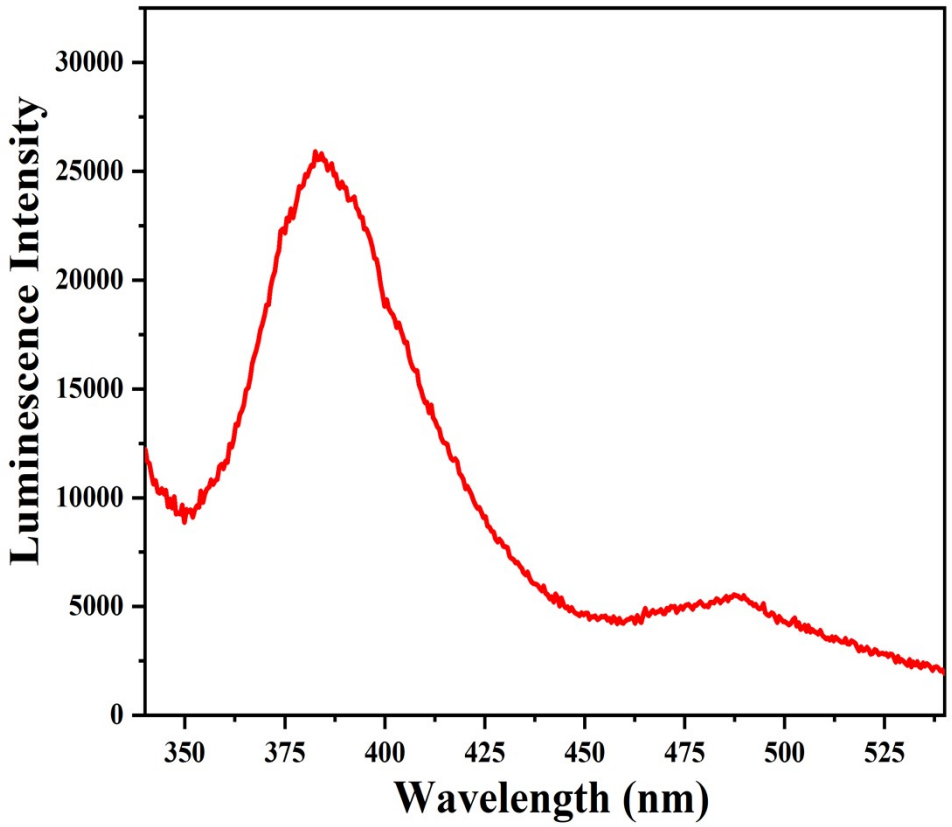

Fig. S18: Emission spectra of 2,4,5-tri-4-pyridyl-1H-imidazole in solid state (λ_{ex} = 300 nm).

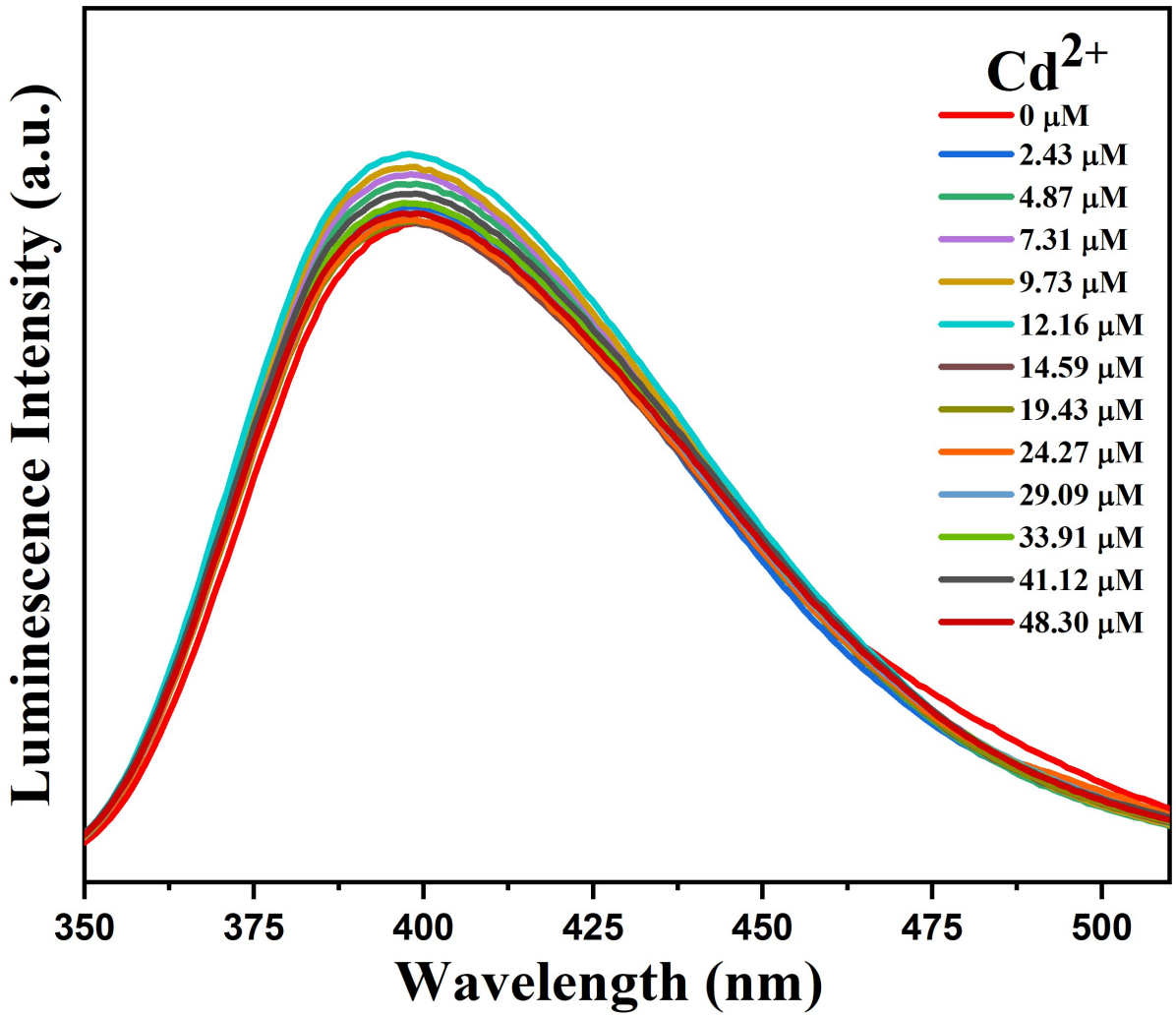

Fig. S19: Emission spectra of **1** dispersed in water upon incremental addition of water solution of Cd^{2+} ions (λ_{ex} = 300 nm). Final concentration of Cd^{2+} ions in the medium is indicated in the legend.

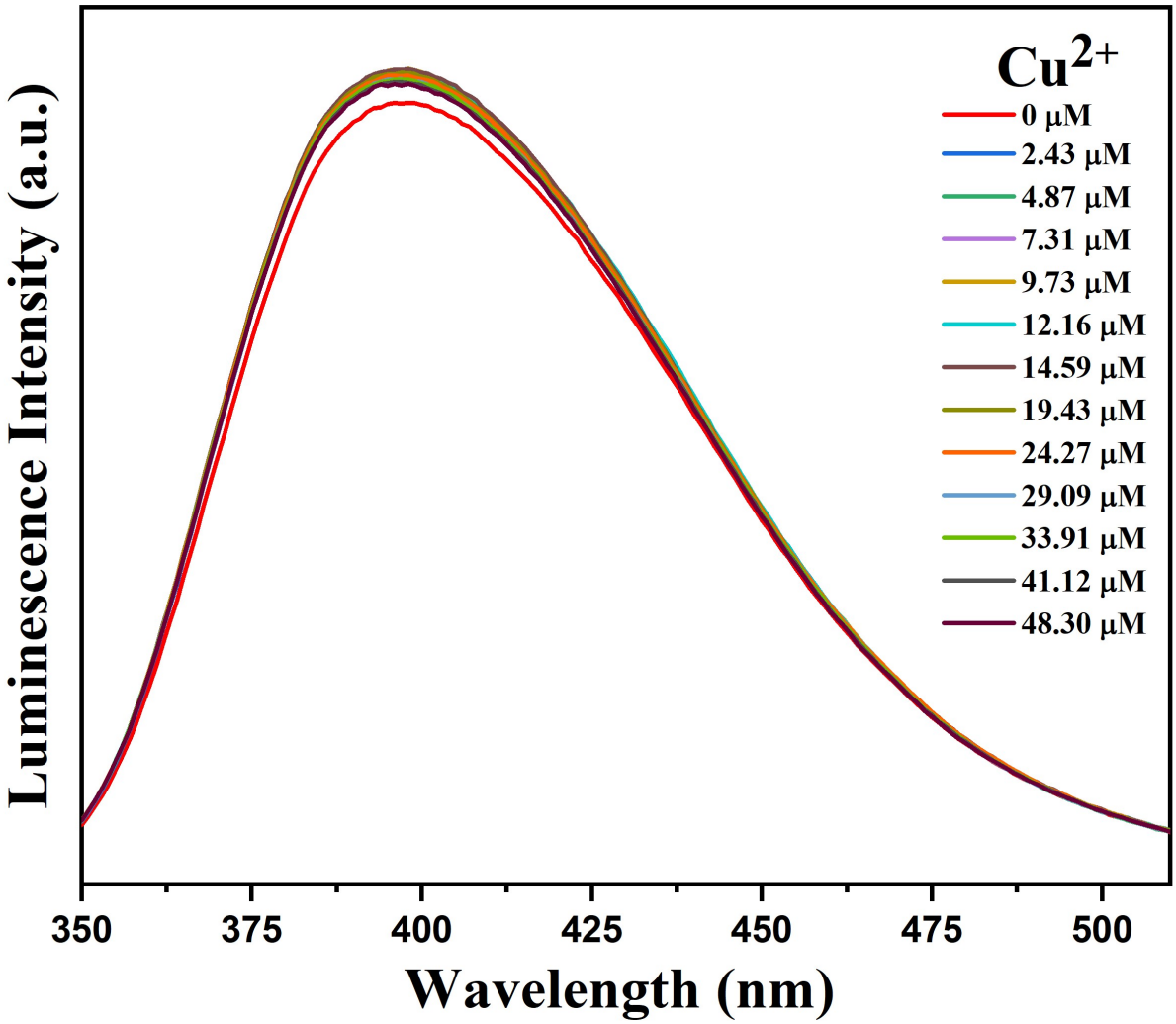

Fig. S20: Emission spectra of **1** dispersed in water upon incremental addition of water solution of Cu^{2+} ions (λ_{ex} = 300 nm). Final concentration of Cu^{2+} ions in the medium is indicated in the legend.

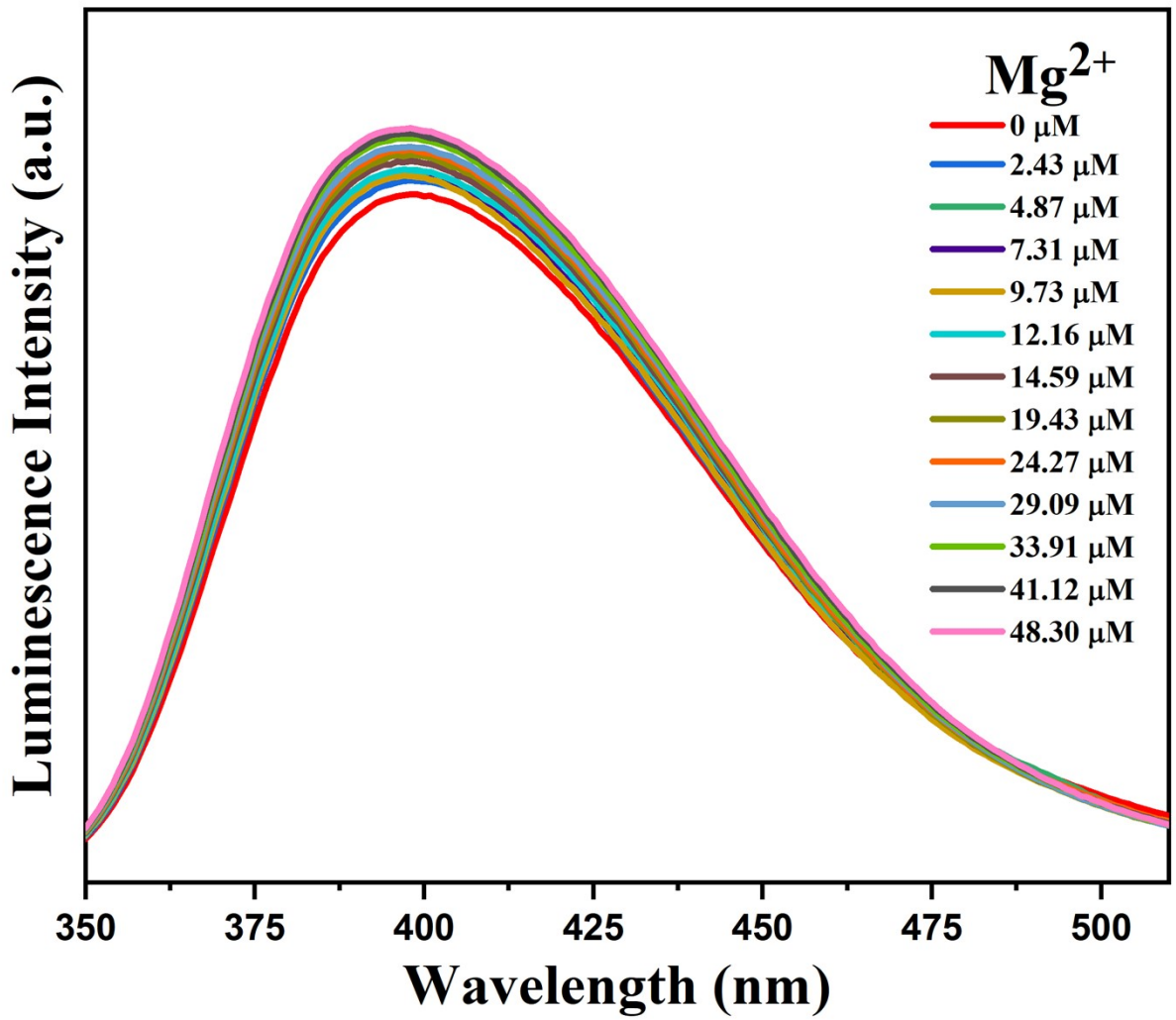

Fig. S21: Emission spectra of **1** dispersed in water upon incremental addition of water solution of Mg^{2+} ions (λ_{ex} = 300 nm). Final concentration of Mg^{2+} ions in the medium is indicated in the legend.

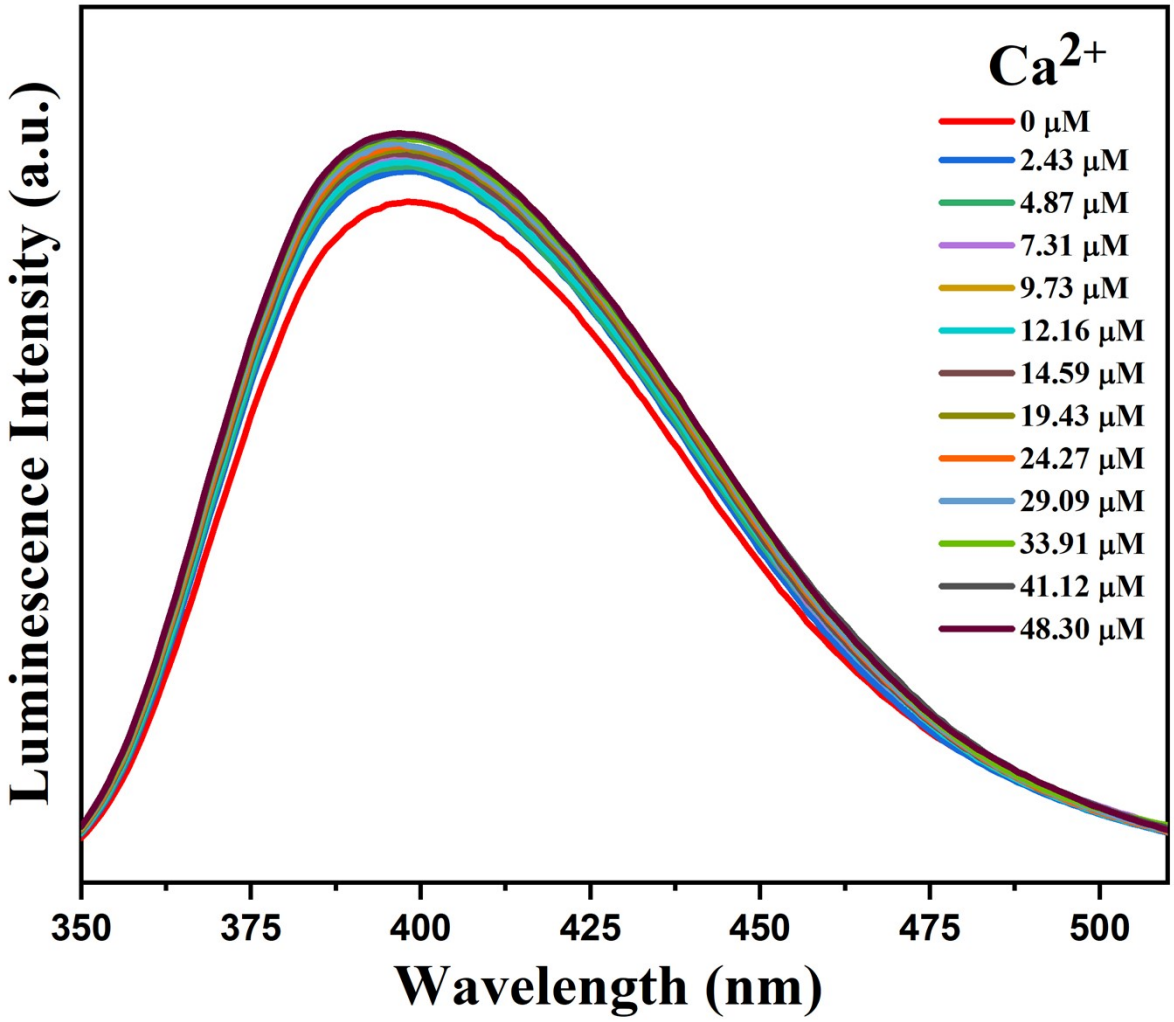

Fig. S22: Emission spectra of **1** dispersed in water upon incremental addition of water solution of Ca^{2+} ions (λ_{ex} = 300 nm). Final concentration of Ca^{2+} ions in the medium is indicated in the legend.

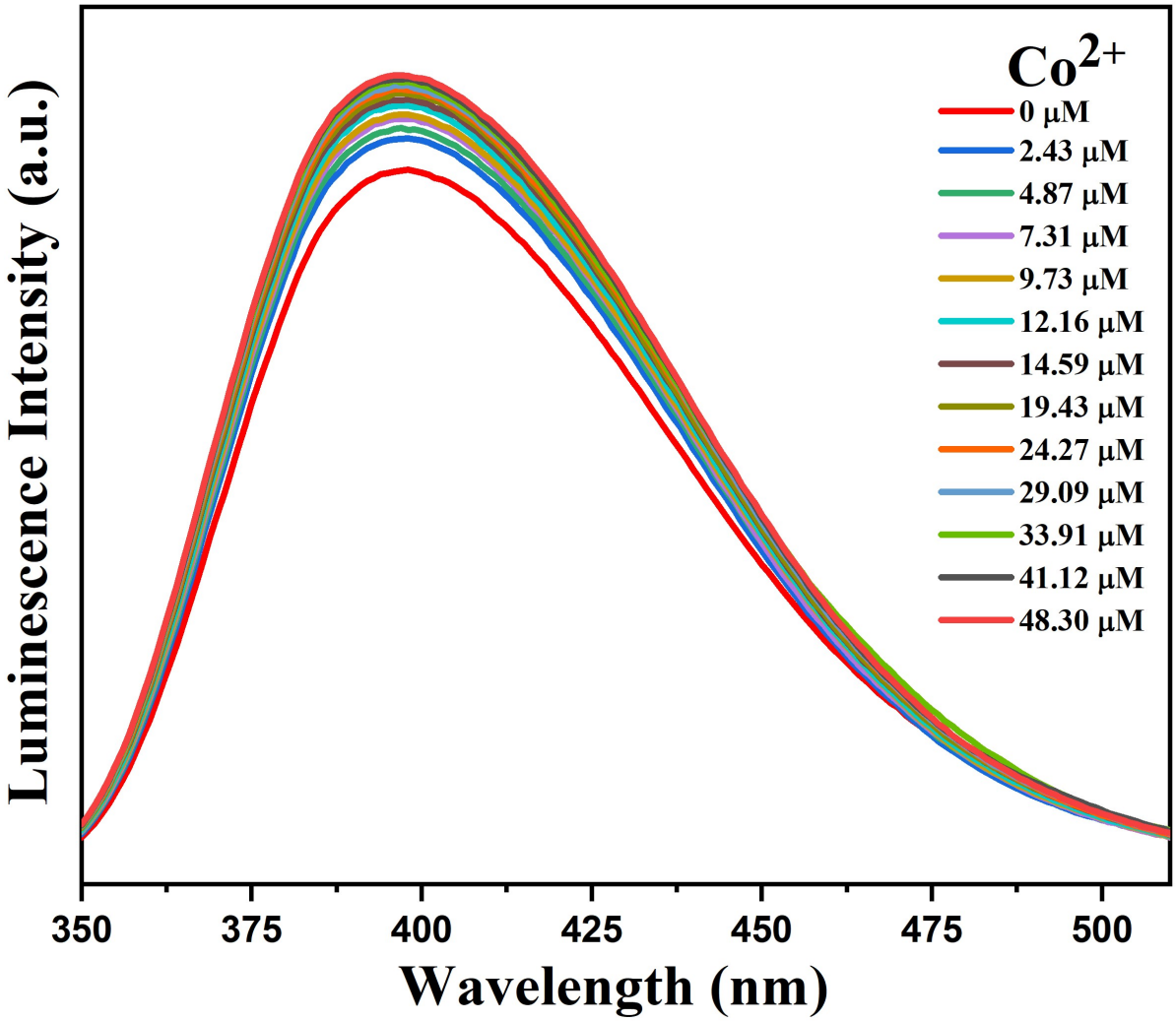

Fig. S23: Emission spectra of **1** dispersed in water upon incremental addition of water solution of Co^{2+} ions (λ_{ex} = 300 nm). Final concentration of Co^{2+} ions in the medium is indicated in the legend.

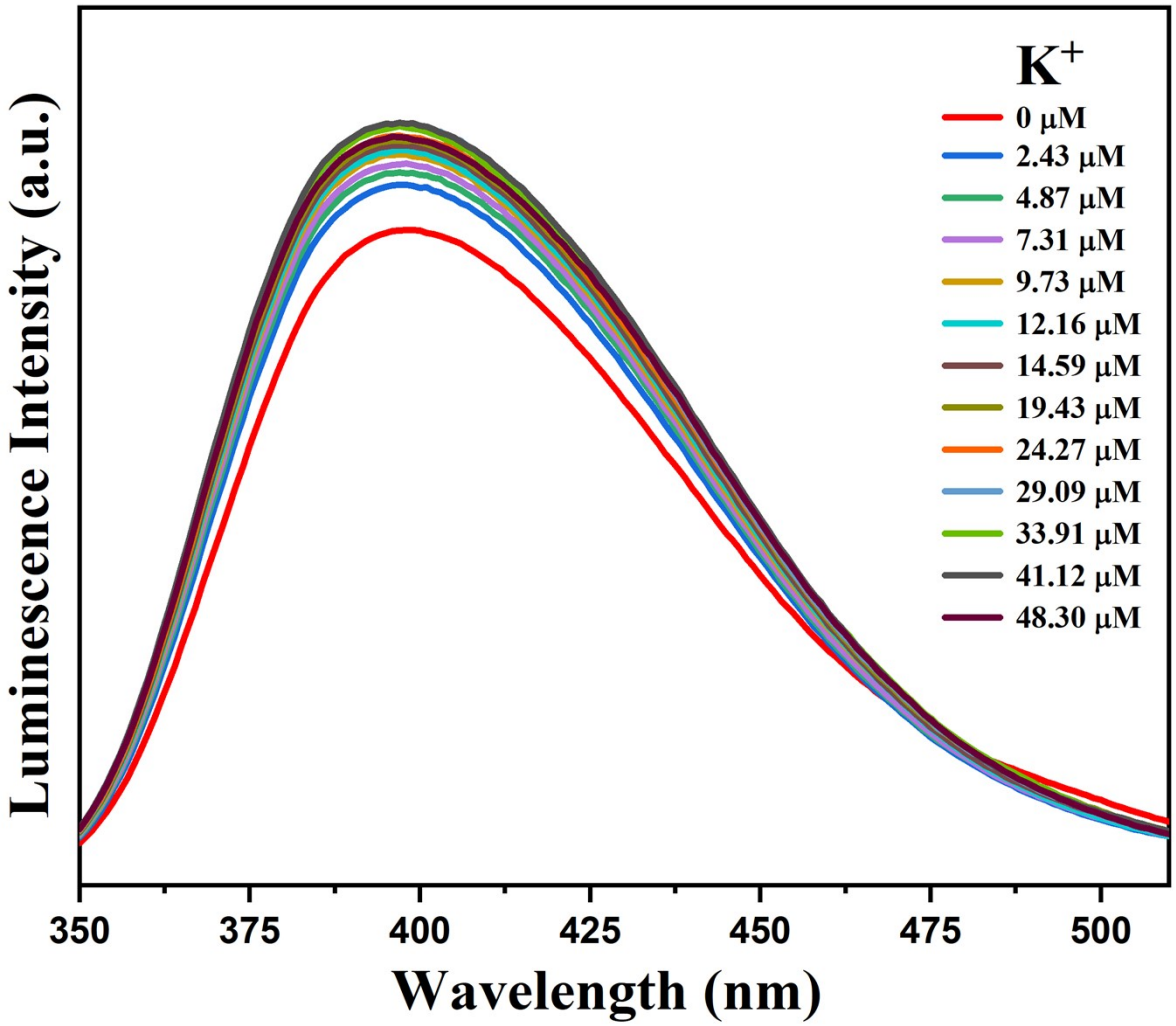

Fig. S24: Emission spectra of **1** dispersed in water upon incremental addition of water solution of K^+ ions (λ_{ex} = 300 nm). Final concentration of K^+ ions in the medium is indicated in the legend.

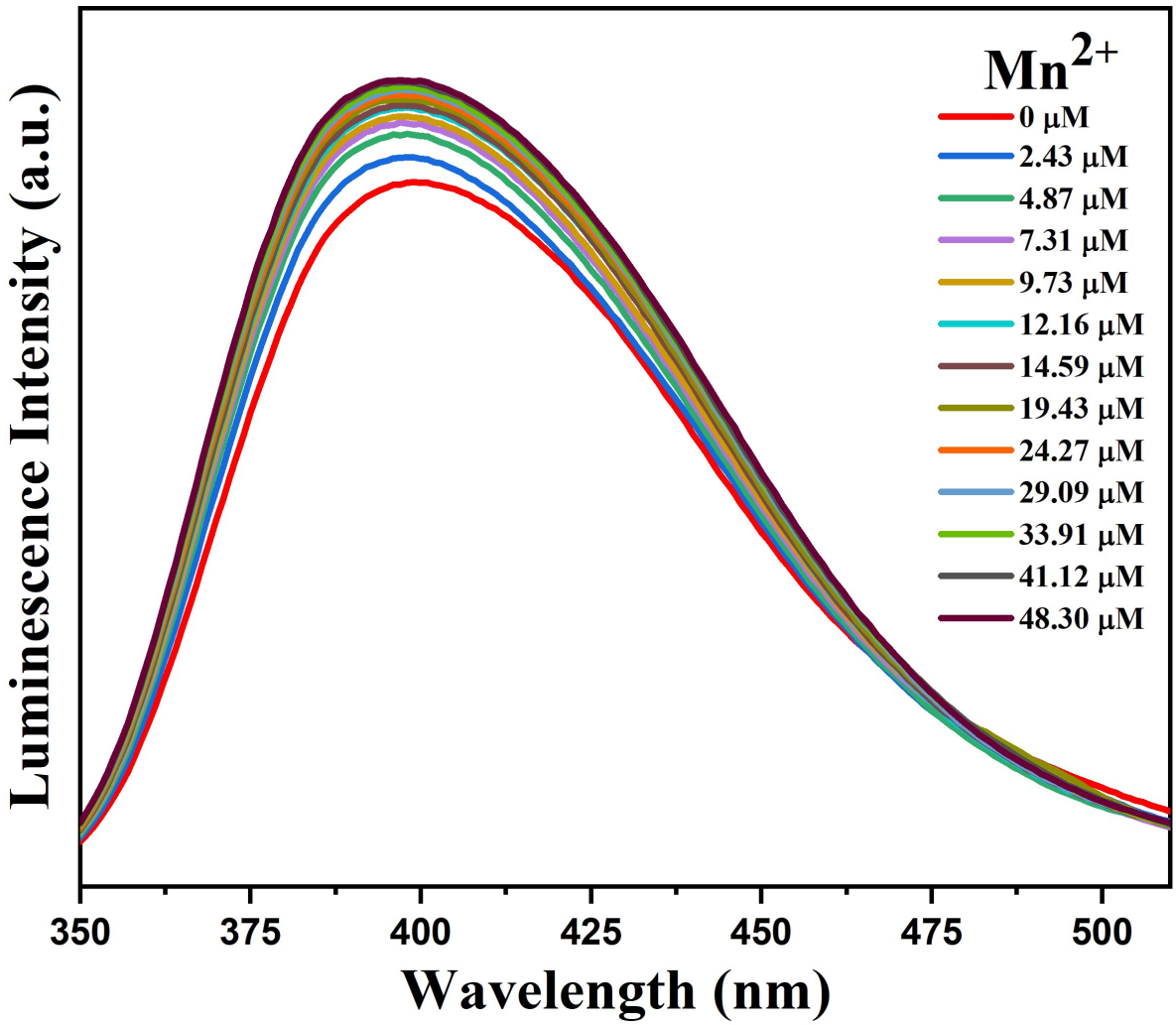

Fig. S25: Emission spectra of **1** dispersed in water upon incremental addition of water solution of Mn^{2+} ions (λ_{ex} = 300 nm). Final concentration of Mn^{2+} ions in the medium is indicated in the legend.

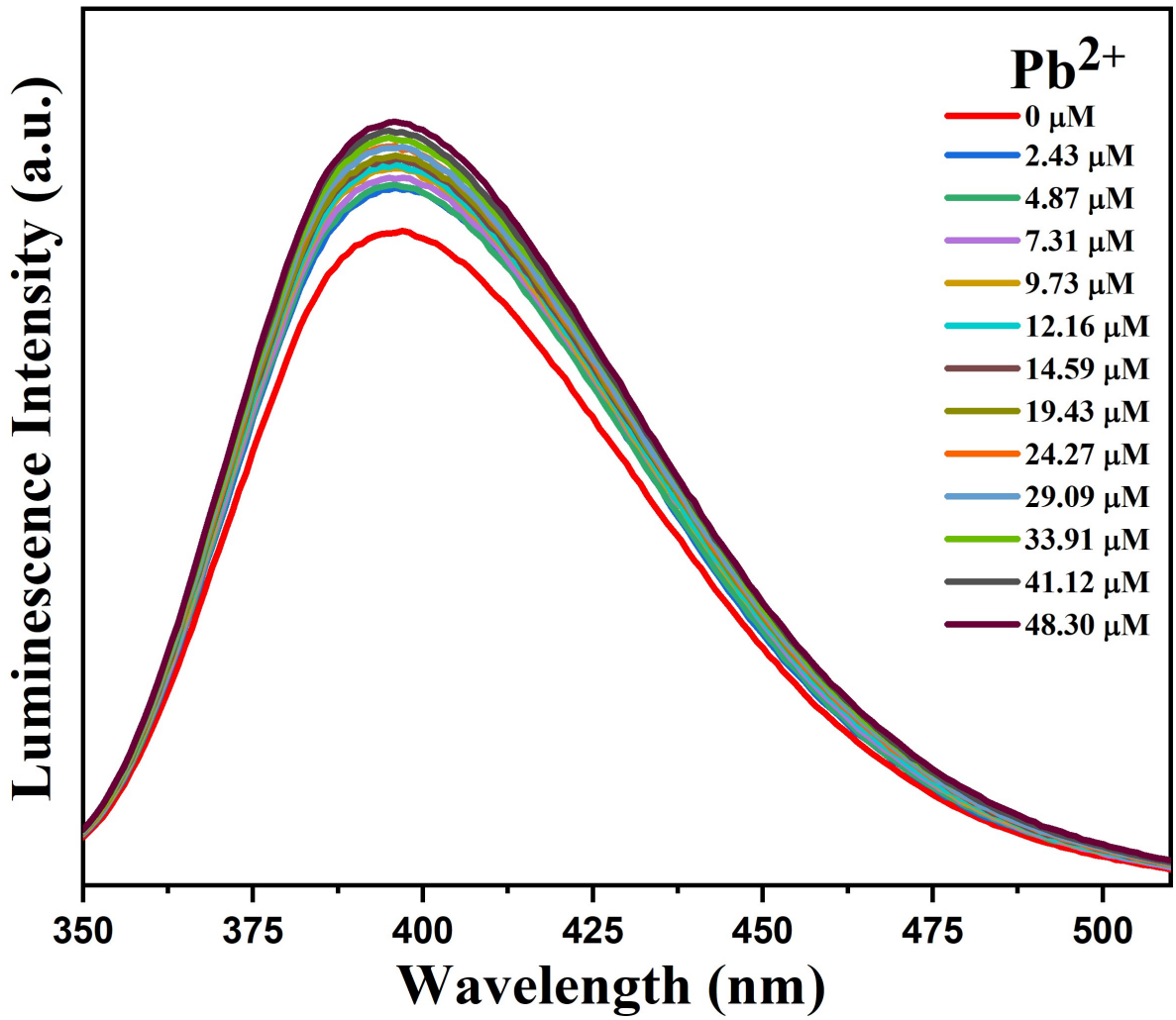

Fig. S26: Emission spectra of **1** dispersed in water upon incremental addition of water solution of Pb^{2+} ions (λ_{ex} = 300 nm). Final concentration of Pb^{2+} ions in the medium is indicated in the legend.

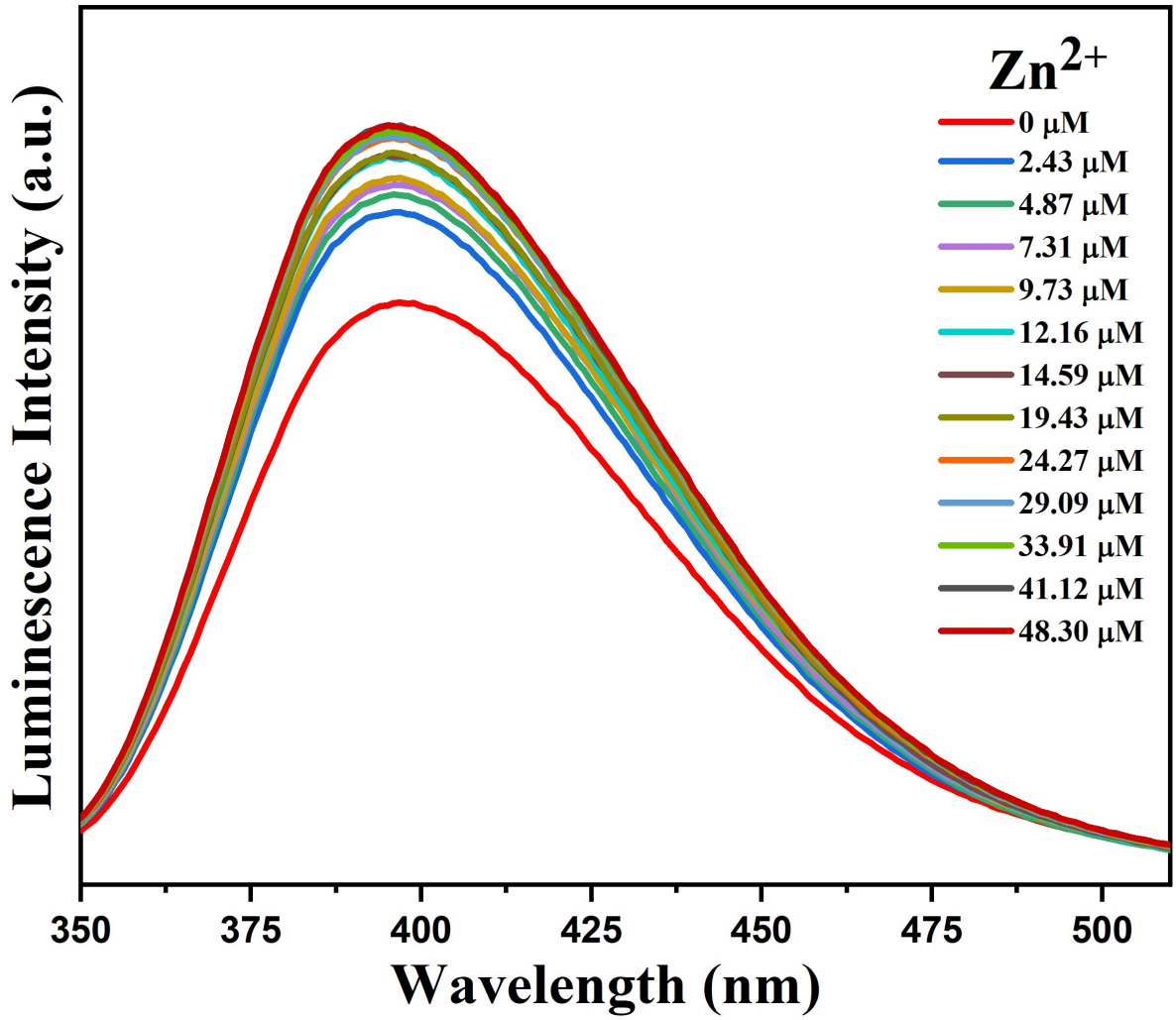

Fig. S27: Emission spectra of **1** dispersed in water upon incremental addition of water solution of Zn^{2+} ions (λ_{ex} = 300 nm). Final concentration of Zn^{2+} ions in the medium is indicated in the legend.

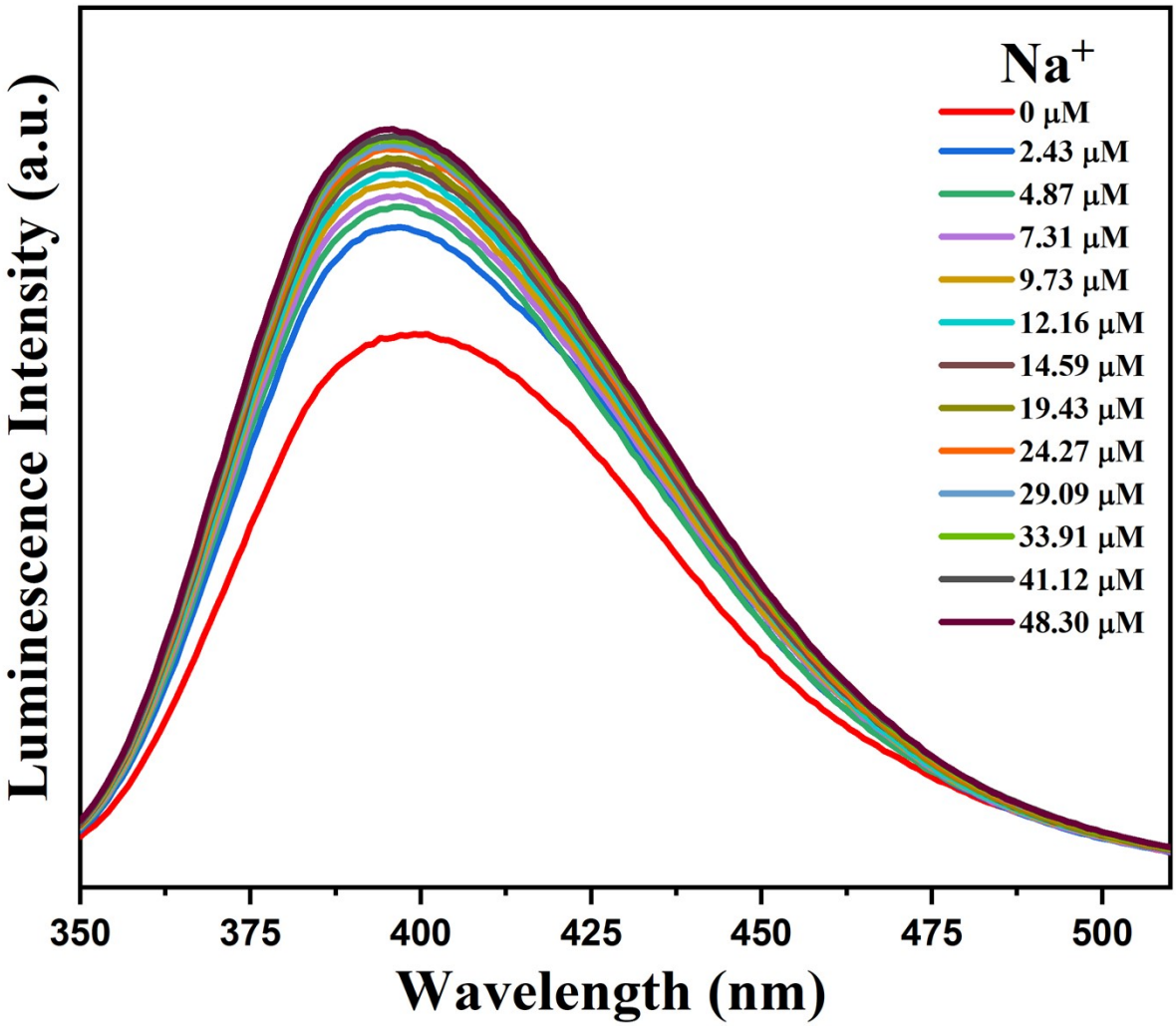

Fig. S28: Emission spectra of **1** dispersed in water upon incremental addition of water solution of Na^+ ions (λ_{ex} = 300 nm). Final concentration of Na^+ ions in the medium is indicated in the legend.

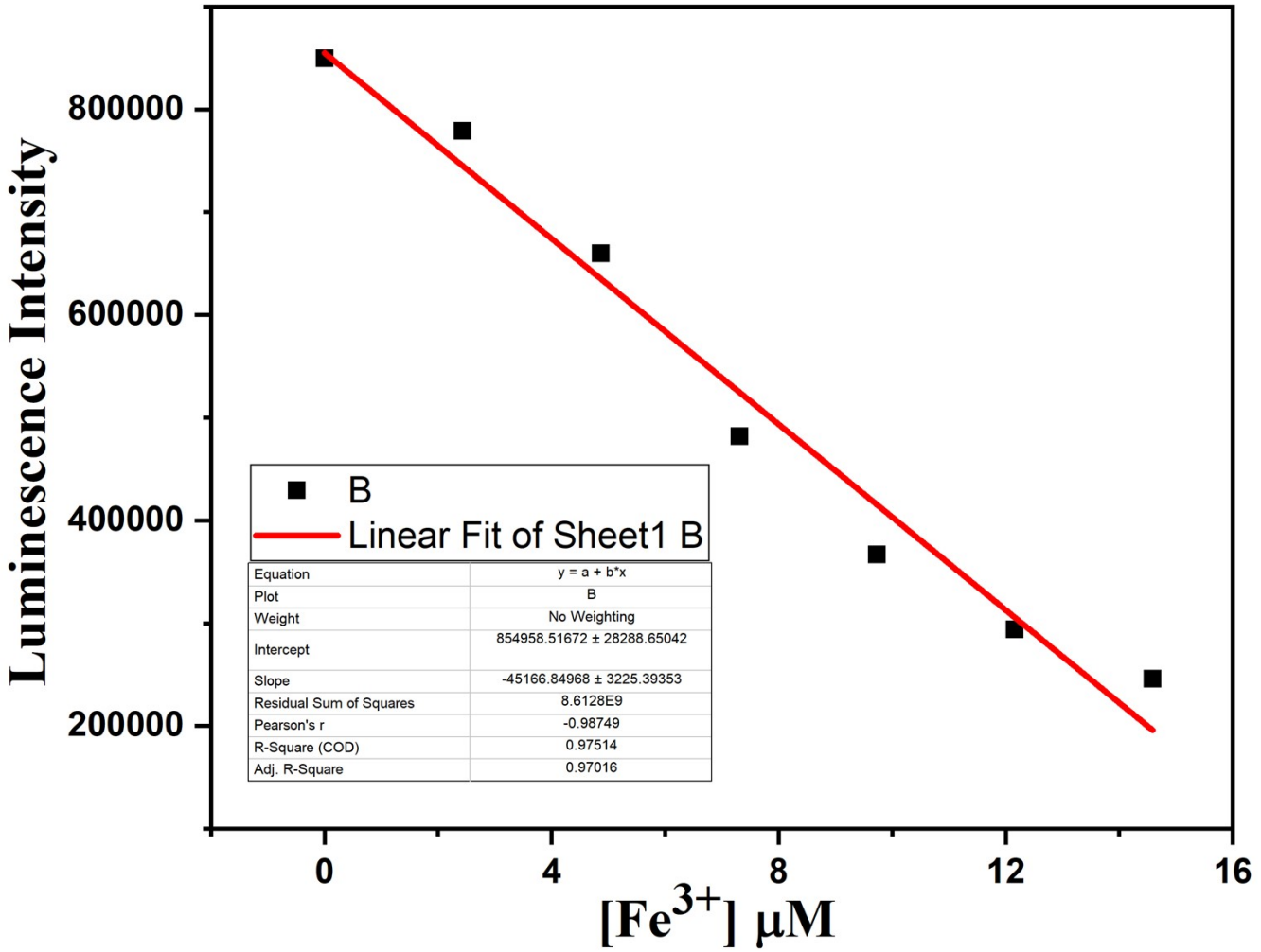

Fig. S29: The plot of the changes of luminescence intensity of compound **1** (λ_{em} = 398 nm) vs concentration of Fe^{3+} solution (upto 14.59 µM) indicating the detection limit, which calculated using the equation, LOD = 3σ/m, where σ = standard deviation of blank determination and m = slope of the linear curve.

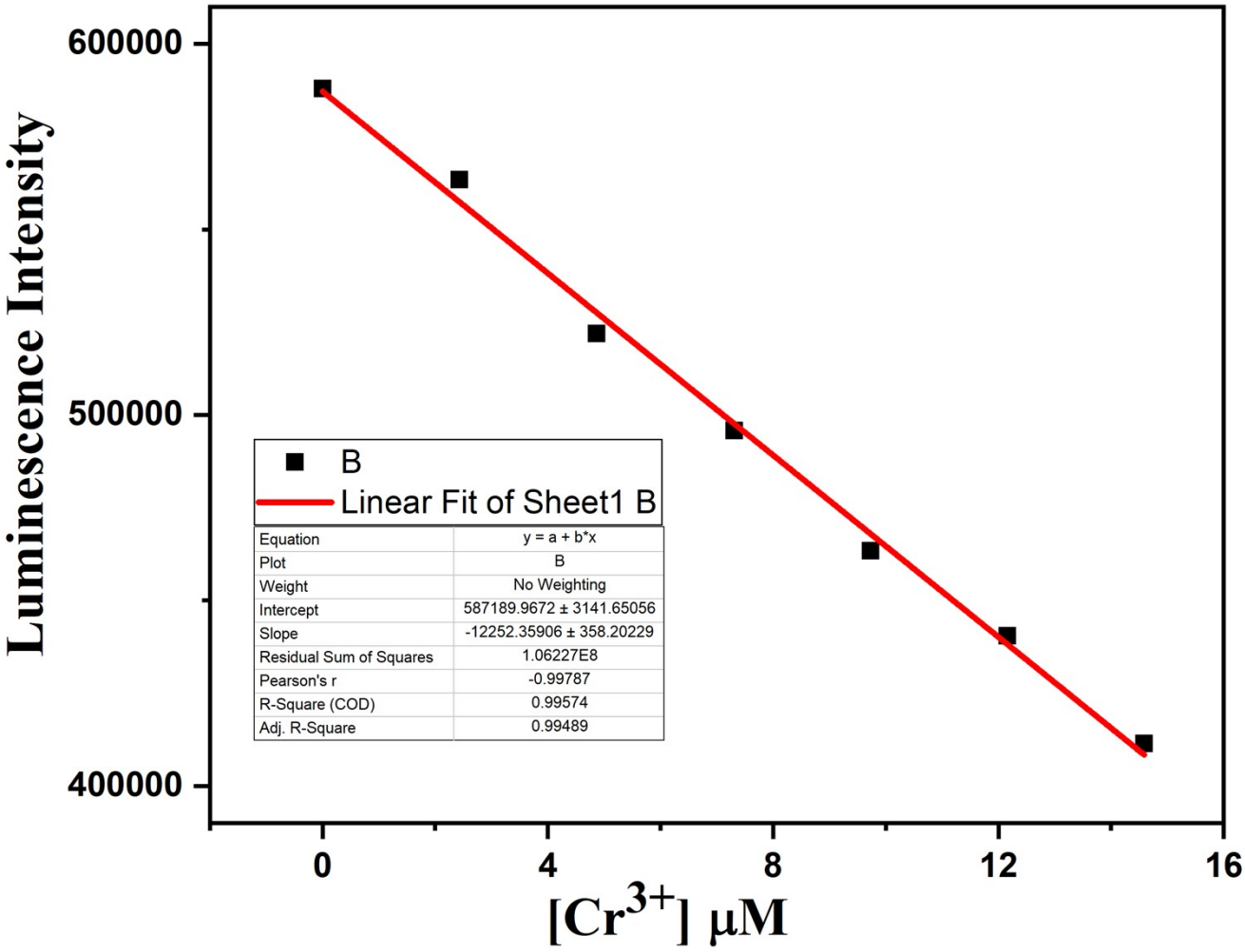

Fig. S30: The plot of the changes of luminescence intensity of compound **1** (λ_{em} = 398 nm) vs concentration of Cr^{3+} solution (upto 14.59 µM) indicating the detection limit, which calculated using the equation, LOD = 3σ/m, where σ = standard deviation of blank determination and m = slope of the linear curve.

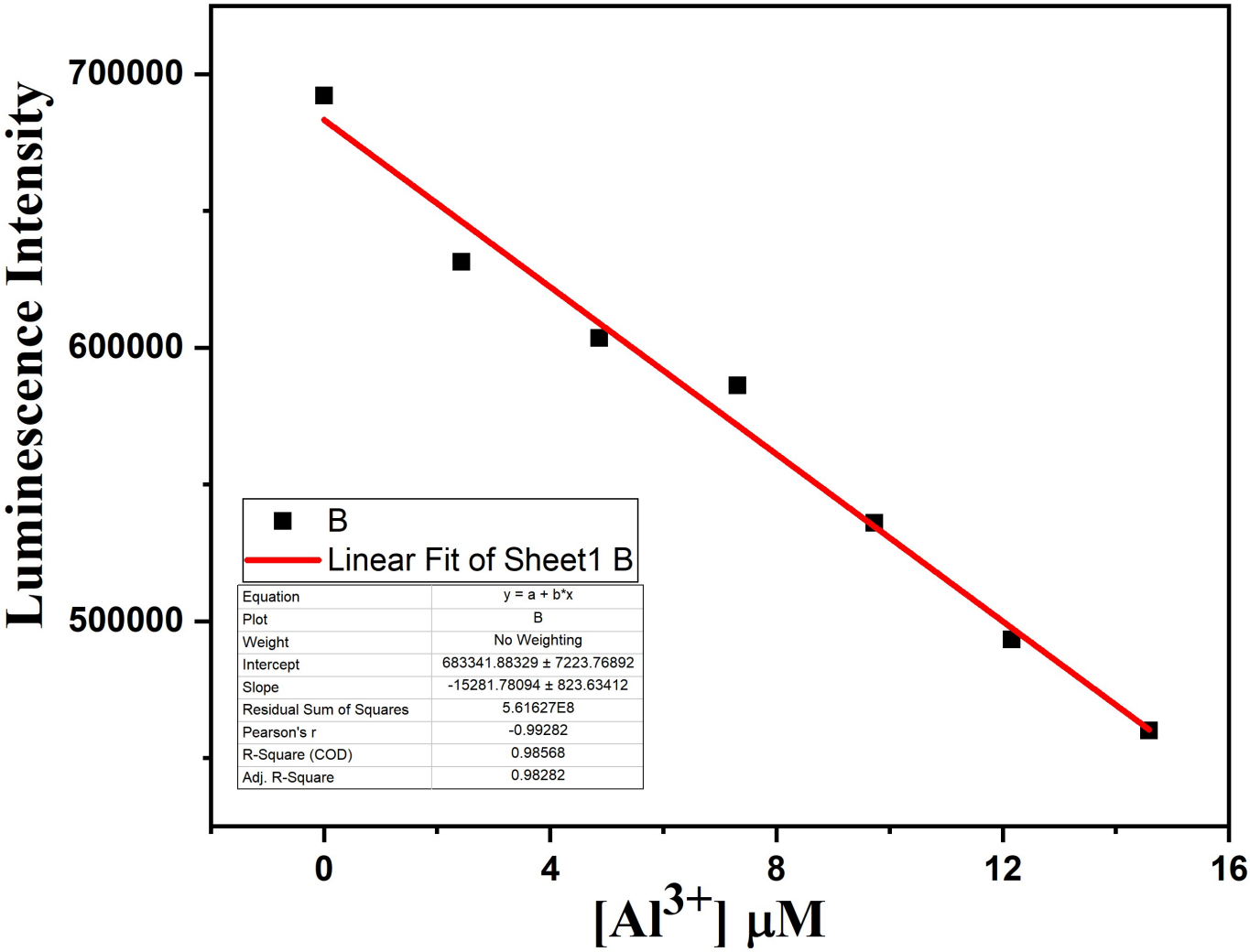

Fig. S31: The plot of the changes of luminescence intensity of compound **1** (λ_{em} = 398 nm) vs concentration of Al^{3+} solution (upto 14.59 µM) indicating the detection limit, which calculated using the equation, LOD = 3σ/m, where σ = standard deviation of blank determination and m = slope of the linear curve.

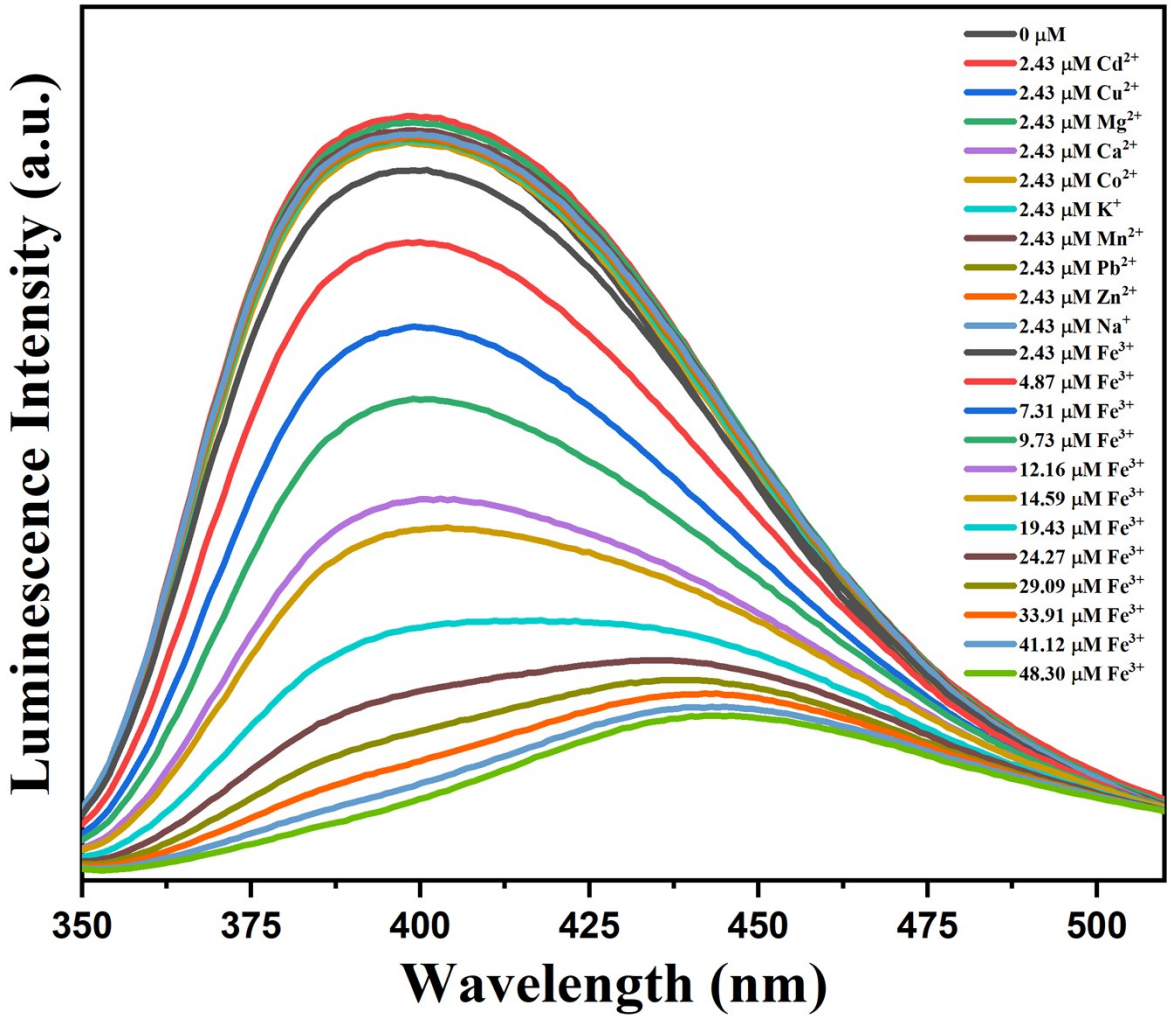

Fig. S32: Emission spectra of **1** dispersed in water upon incremental addition of Fe^{3+}solution in the presence of 2.43 μM concentration of various metal ions (λ_{ex} = 300 nm).

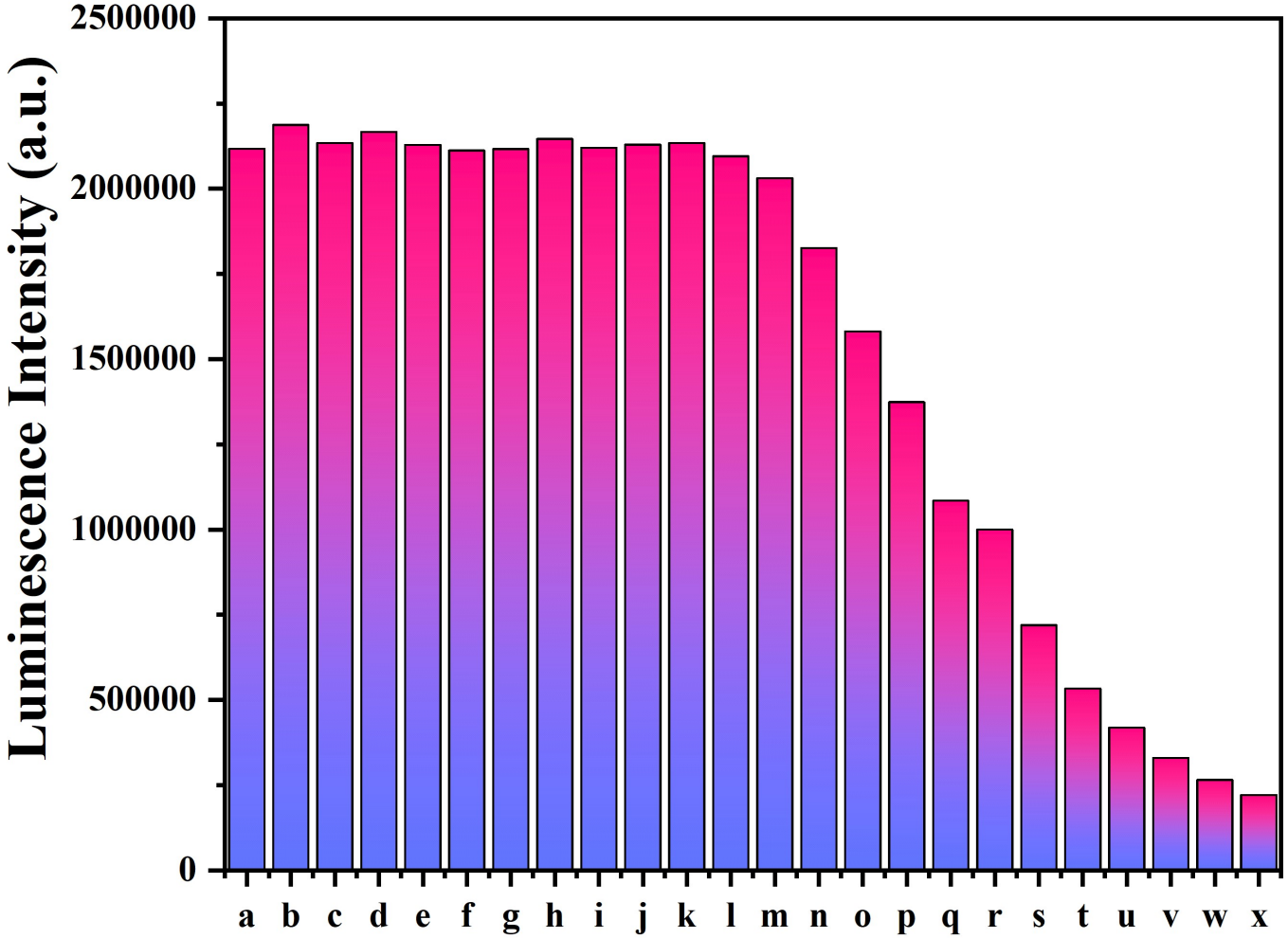

Fig. S33: Bar diagram presenting the luminescence intensity (observed at 398 nm) after the consecutive addition of the analytes. The composition and concentration of the system were as follows: (a) **1** in aqueous dispersion, (b) a + 2.43 μM Cd^{2+}, (c) b + 2.43 μM Cu^{2+}, (d) c + 2.43 μM Mg^{2+}, (e) d + 2.43 μM Ca^{2+}, (f) e + 2.43 μM Co^{2+}, (g) f + 2.43 μM K^{+}, (h) g + 2.43 μM Mn^{2+}, (i) h + 2.43 μM Pb^{2+}, (j) i + 2.43 μM Zn^{2+}, (k) j + 2.43 μM Na^{+}, (l) k + 2.43 μM Fe^{3+}, (m) l + 2.43 μM Fe^{3+}, (n) m + 2.43 μM Fe^{3+}, (o) n + 2.43 μM Fe^{3+}, (p) o + 2.43 μM Fe^{3+}, (q) p + 2.43 μM Fe^{3+}, (r) q + 4.87 μM Fe^{3+}, (s) r + 4.87 μM Fe^{3+}, (t) s + 4.87 μM Fe^{3+}, (u) q + 4.87 μM Fe^{3+}, (v) r + 4.87 μM Fe^{3+}, (w) s + 7.31 μM Fe^{3+}, and (x) s + 7.31 μM Fe^{3+}.

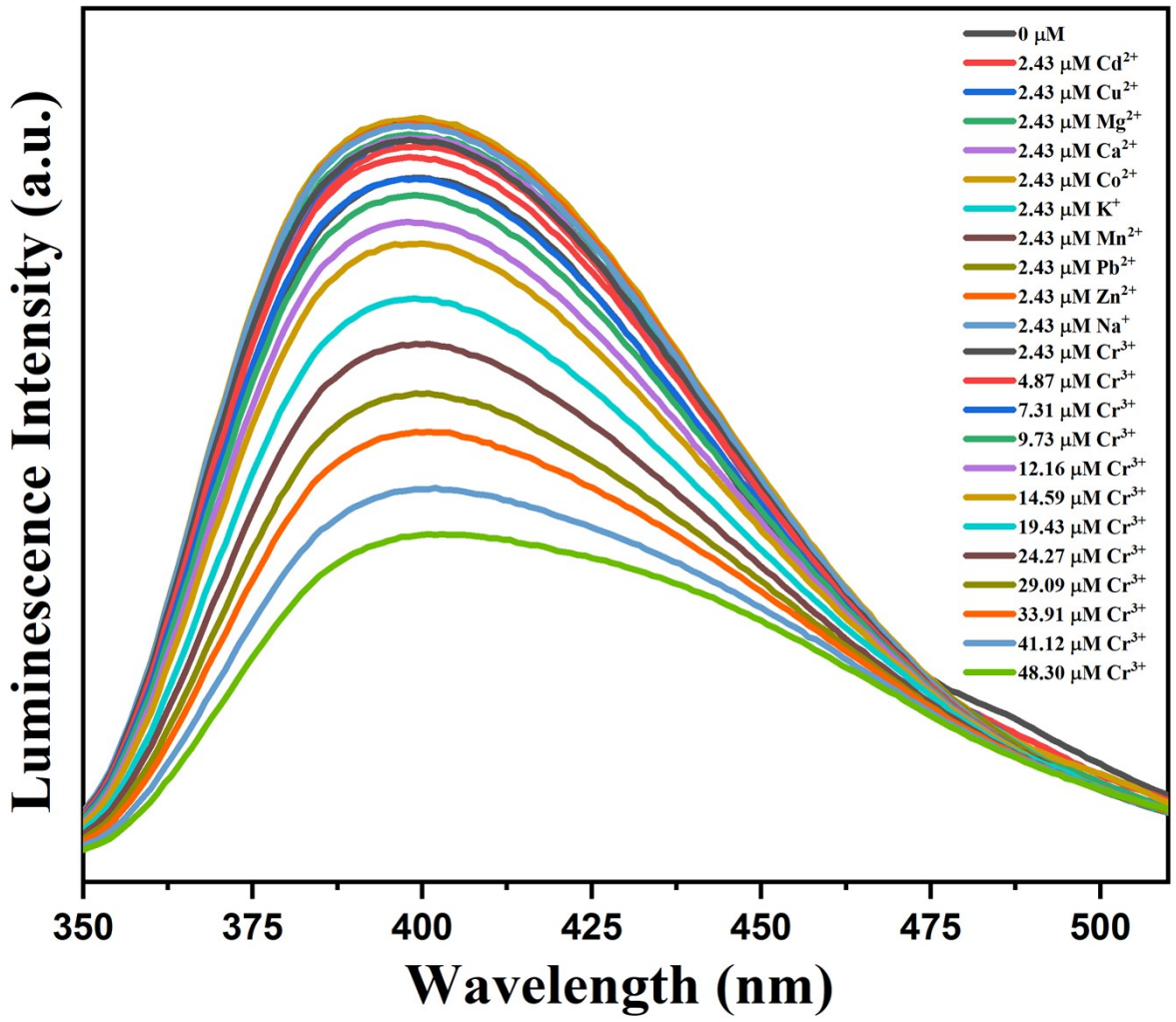

Fig. S34: Emission spectra of **1** dispersed in water upon incremental addition of Cr^{3+}solution in the presence of 2.43 μM concentration of various metal ions (λ_{ex} = 300 nm).

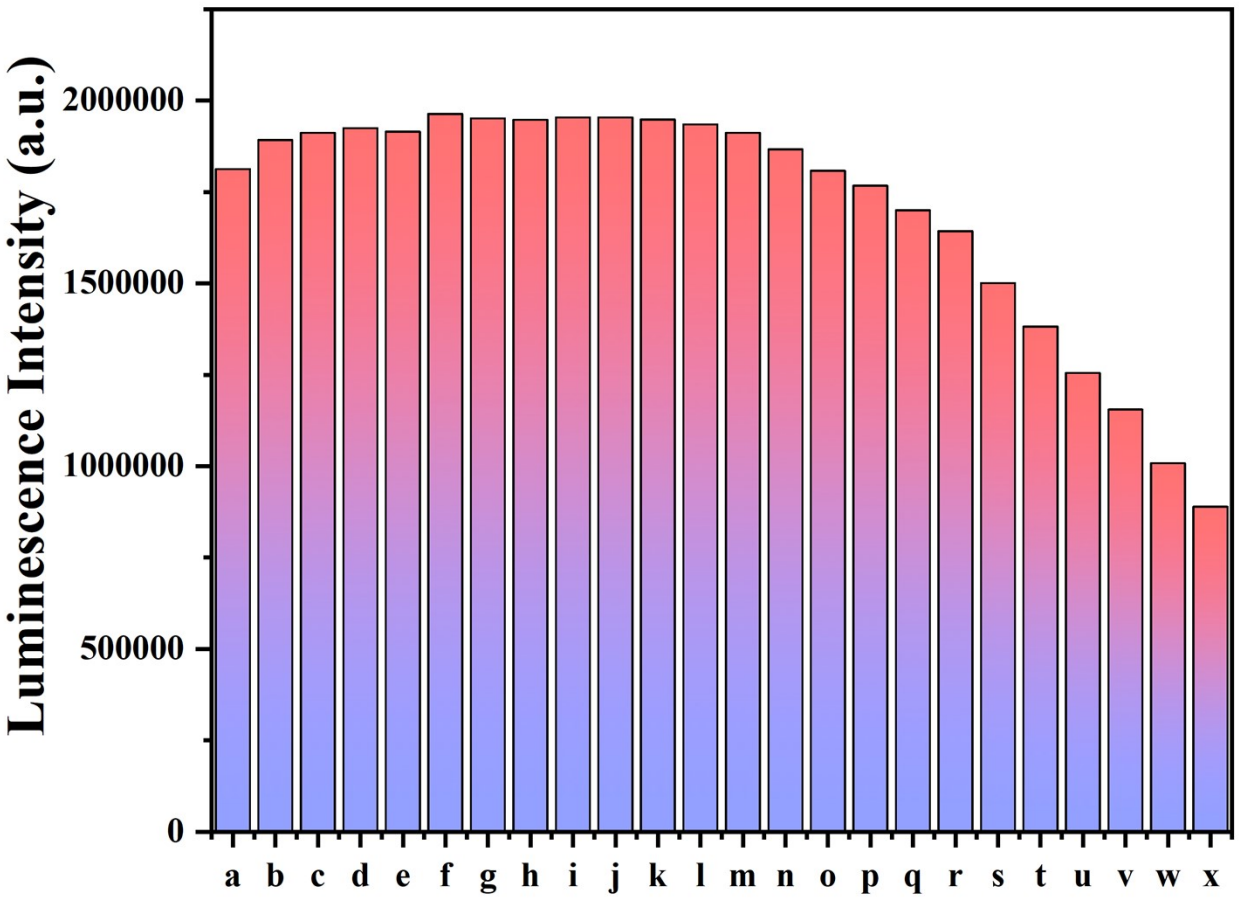

Fig. S35: Bar diagram presenting the luminescence intensity (observed at 398 nm) after the consecutive addition of the analytes. The composition and concentration of the system were as follows: (a) **1** in aqueous dispersion, (b) a + 2.43 μM Cd^{2+}, (c) b + 2.43 μM Cu^{2+}, (d) c + 2.43 μM Mg^{2+}, (e) d + 2.43 μM Ca^{2+}, (f) e + 2.43 μM Co^{2+}, (g) f + 2.43 μM K^{+}, (h) g + 2.43 μM Mn^{2+}, (i) h + 2.43 μM Pb^{2+}, (j) i + 2.43 μM Zn^{2+}, (k) j + 2.43 μM Na^{+}, (l) k + 2.43 μM Cr^{3+}, (m) l + 2.43 μM Cr^{3+}, (n) m + 2.43 μM Cr^{3+}, (o) n + 2.43 μM Cr^{3+}, (p) o + 2.43 μM Cr^{3+}, (q) p + 2.43 μM Cr^{3+}, (r) q + 4.87 μM Cr^{3+}, (s) r + 4.87 μM Cr^{3+}, (t) s + 4.87 μM Cr^{3+}, (u) q + 4.87 μM Cr^{3+}, (v) r + 4.87 μM Cr^{3+}, (w) s + 7.31 μM Cr^{3+}, and (x) s + 7.31 μM Cr^{3+}.

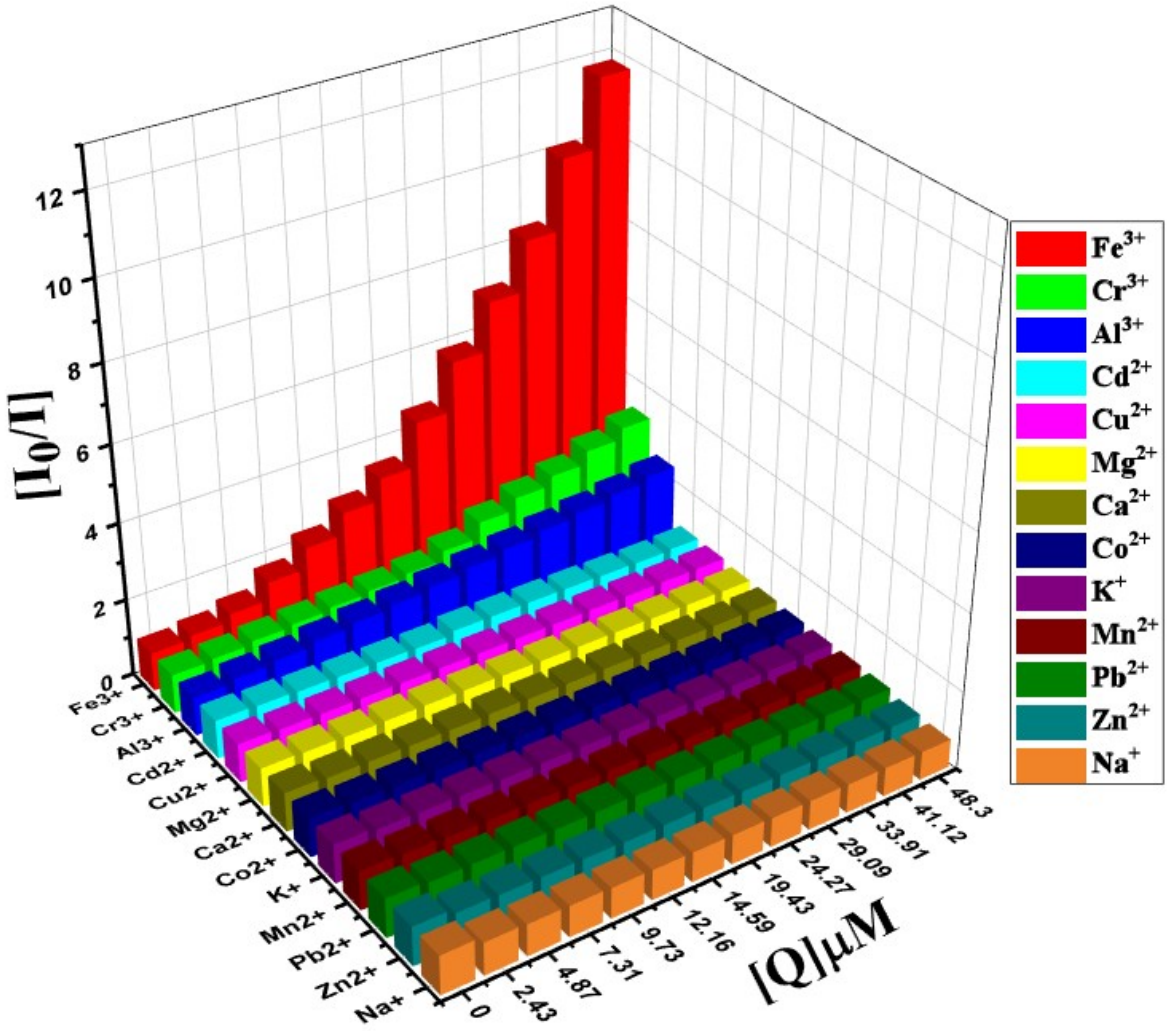

Fig. 36: Stern-Volmer plots of various metal ions in higher concentration range (upto 48.30 μM) for compound **1**.

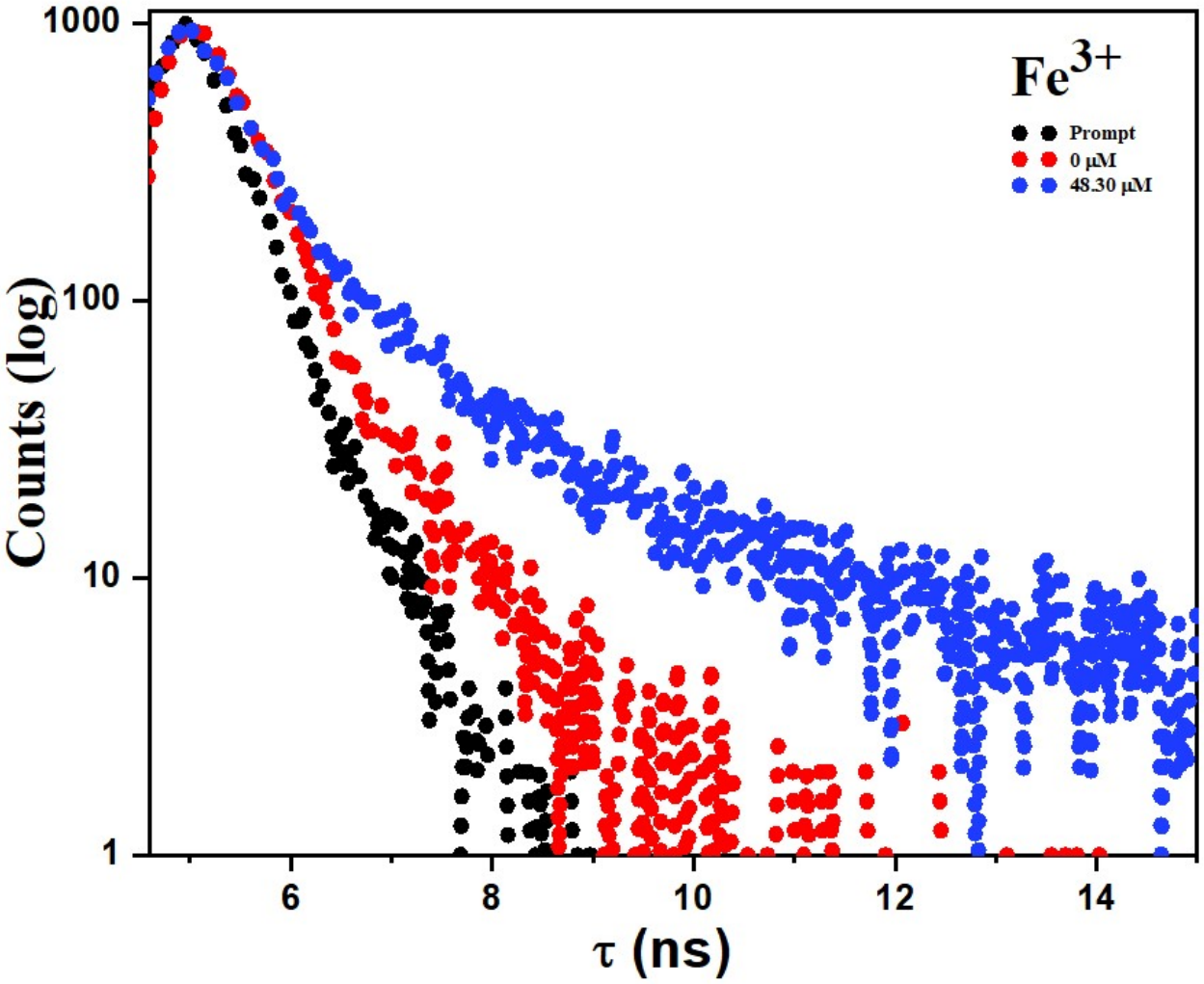

Fig. S37: Luminescence lifetime decay profile of compound **1** before and after the addition of the Fe^{3+} ions. The final concentration of Fe^{3+} ions in the medium is indicated in the legend. The instrument response function (prompt) is also shown. Here, λ_{ex} = 300 nm and λ_{em} = 398 nm were set during the experiment.

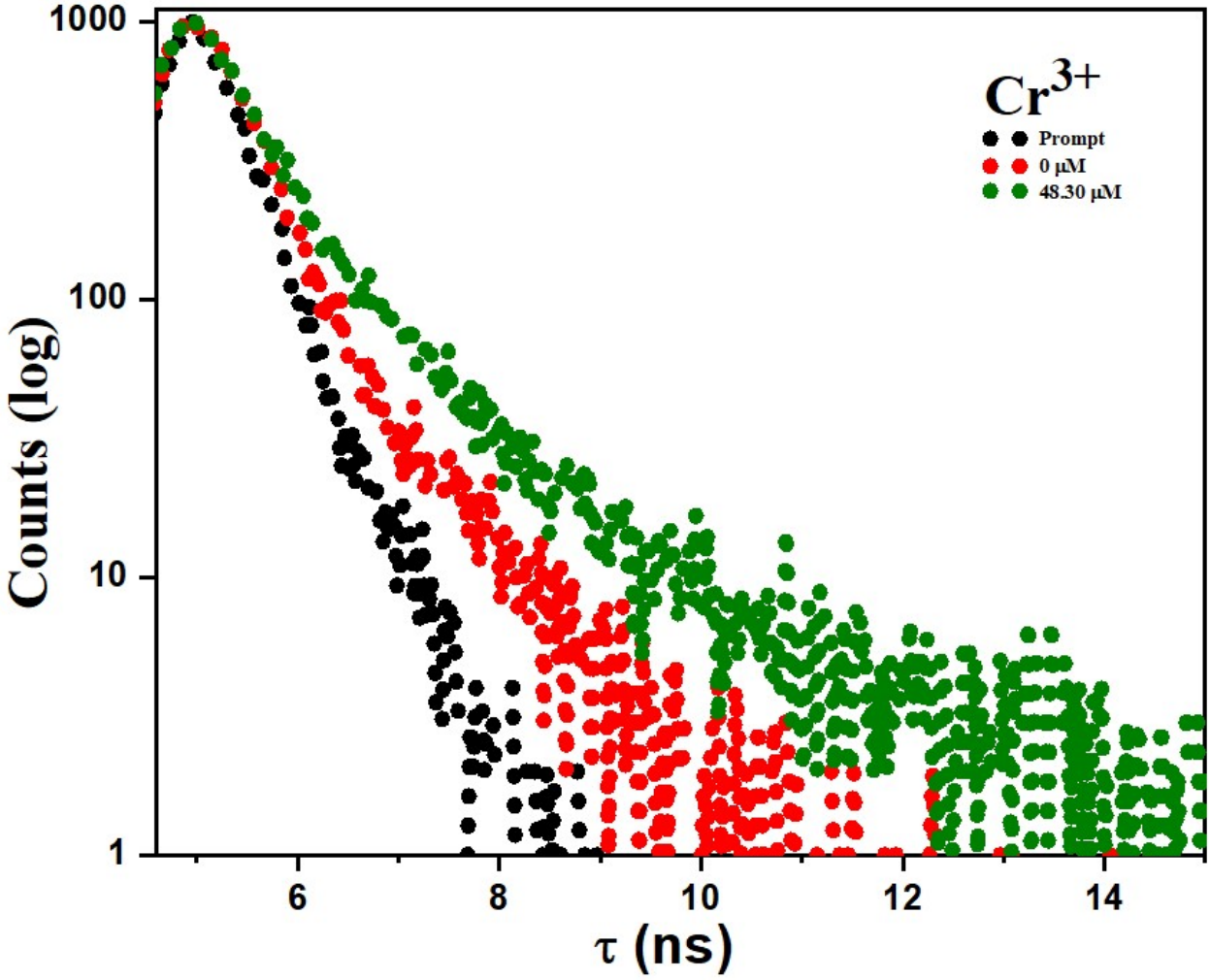

Fig. S38: Luminescence lifetime decay profile of compound **1** before and after the addition of the Cr^{3+} ions. The final concentration of Cr^{3+} ions in the medium is indicated in the legend. The instrument response function (prompt) is also shown. Here, λ_{ex} = 300 nm and λ_{em} = 398 nm were set during the experiment.

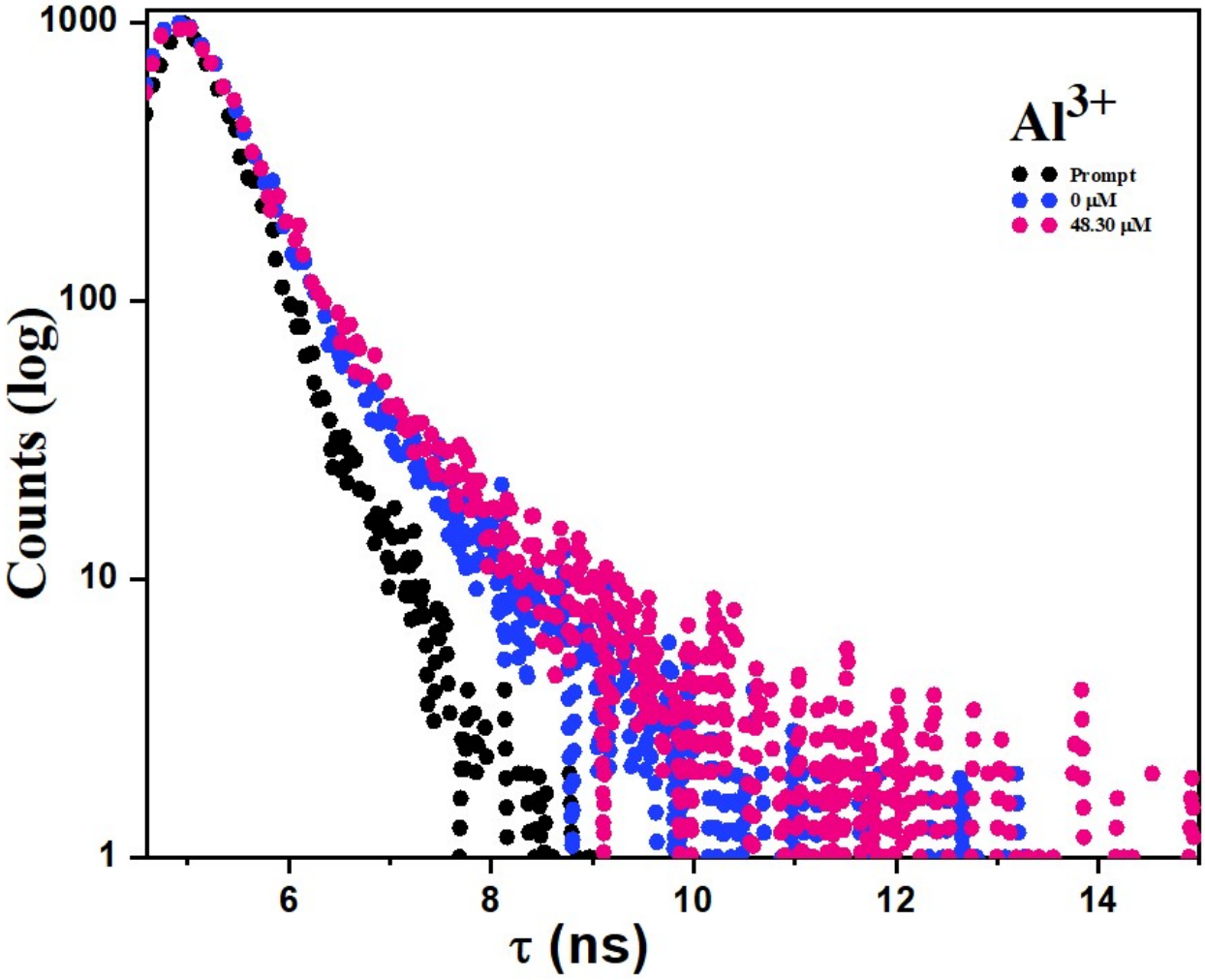

Fig. S39: Luminescence lifetime decay profile of compound **1** before and after the addition of the Al^{3+} ions. The final concentration of Al^{3+} ions in the medium is indicated in the legend. The instrument response function (prompt) is also shown. Here, λ_{ex} = 300 nm and λ_{em} = 398 nm were set during the experiment.

Table S5: Details about the time-resolved luminescence decays of compound **1** (λ_{ex} = 300 nm and λ_{em} = 398 nm) in presence of Fe^{3+}, Cr^{3+}, Al^{3+} solution.

Metal ions	Concentration (μM)	Lifetime (ns)			
		T_1	T_2	$T_{av} = (T_1+T_2)/2$	τ(ns)
Fe^{3+}	0	0.2030	0	0.101	0.203
	48.30	0.1479	1.2854	0.716	0.344
Cr^{3+}	0	0.2321	0	0.116	0.232
	48.30	0.1590	1.3480	0.753	0.490
Al^{3+}	0	0.2415	0	0.120	0.241
	48.30	0.1322	1.0551	0.593	0.301

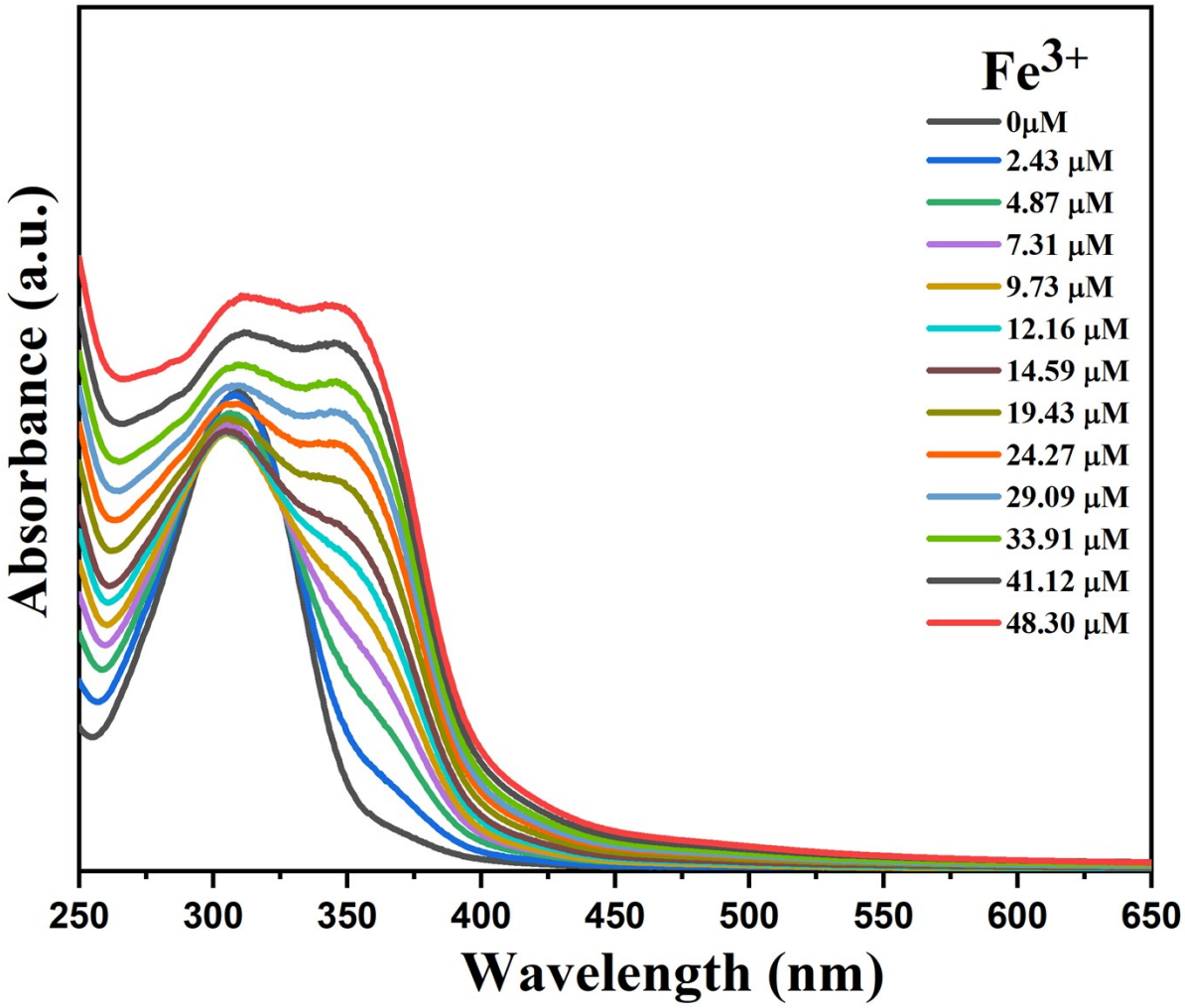

Fig. S40: Absorption spectra of **1** dispersed in water upon incremental addition of water solution of Fe^{3+} ions. Final concentration of Fe^{3+} ions in the medium is indicated in the legend.

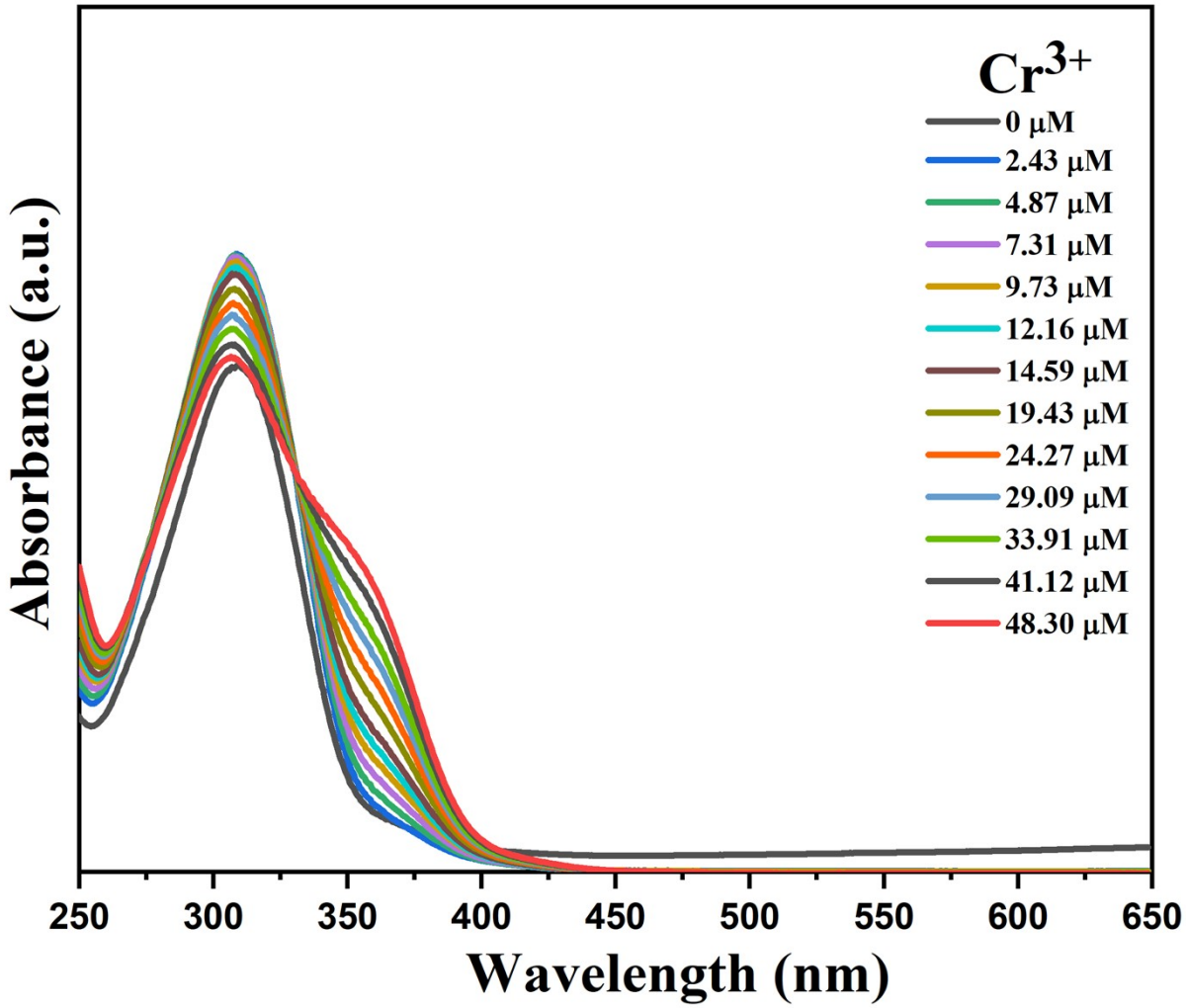

Fig. S41: Absorption spectra of **1** dispersed in water upon incremental addition of water solution of Cr^{3+} ions. Final concentration of Cr^{3+} ions in the medium is indicated in the legend.

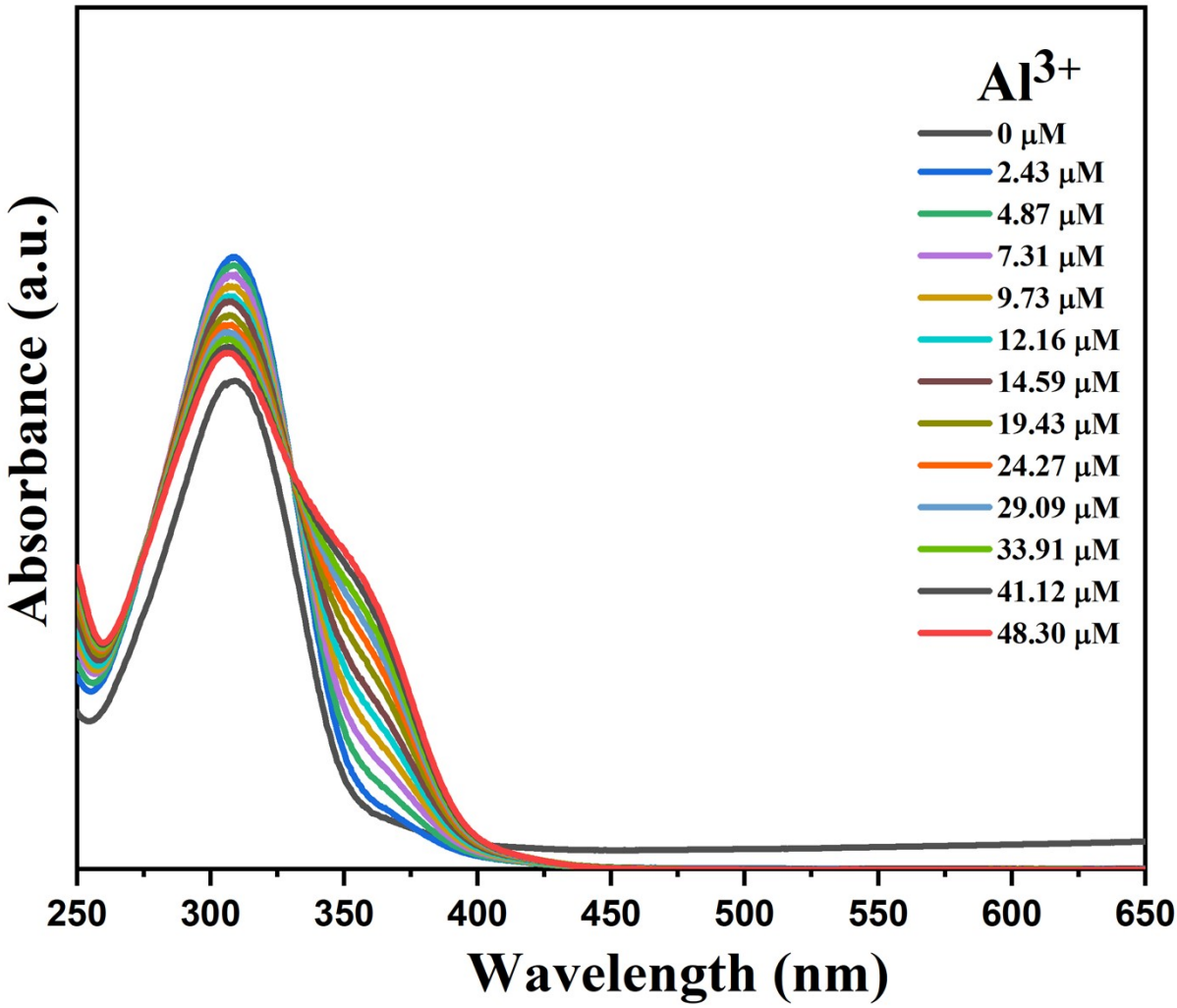

Fig. S42: Absorption spectra of **1** dispersed in water upon incremental addition of water solution of Al^{3+} ions. Final concentration of Al^{3+} ions in the medium is indicated in the legend.

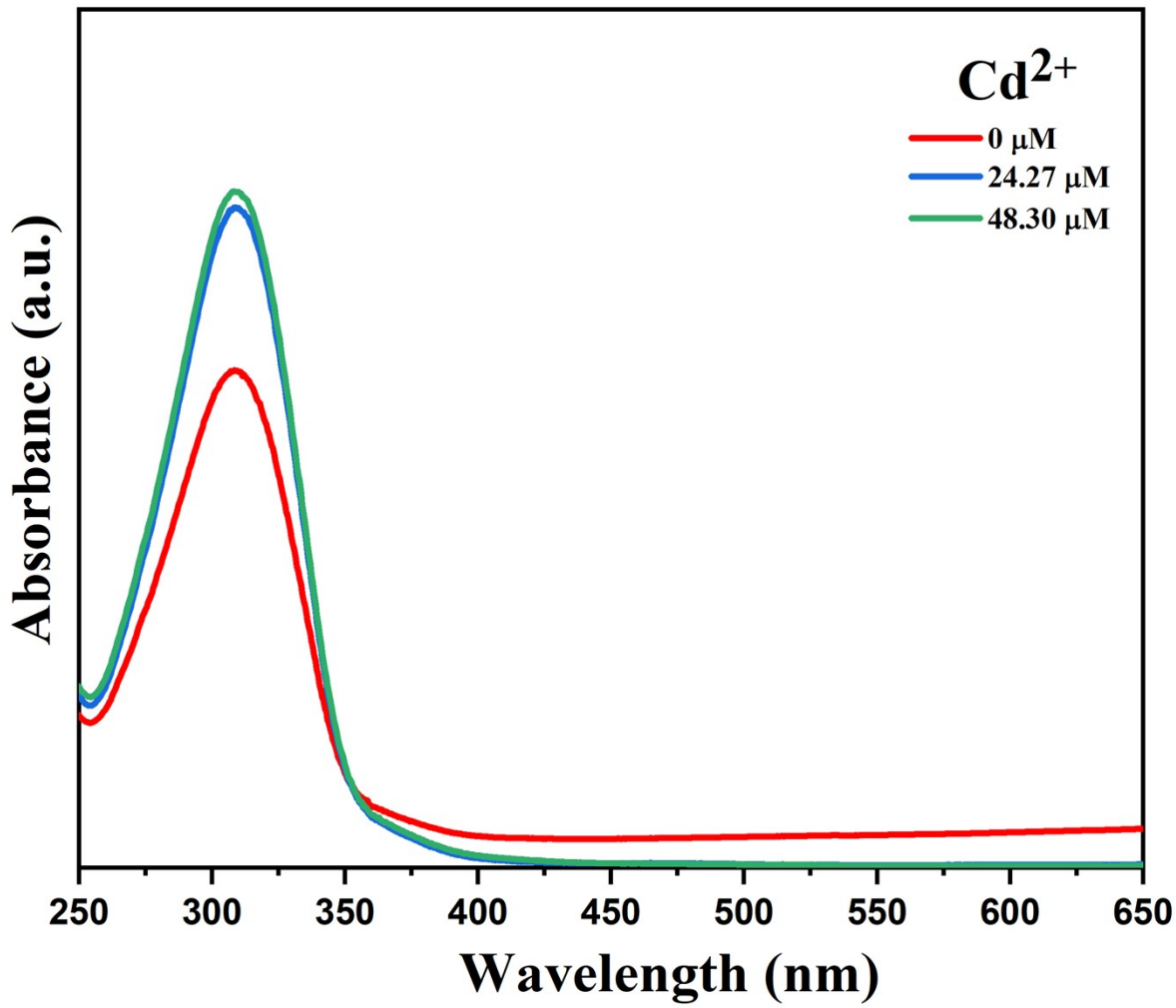

Fig. S43: Absorption spectra of **1** dispersed in water upon incremental addition of water solution of Cd^{2+} ions. Final concentration of Cd^{2+} ions in the medium is indicated in the legend.

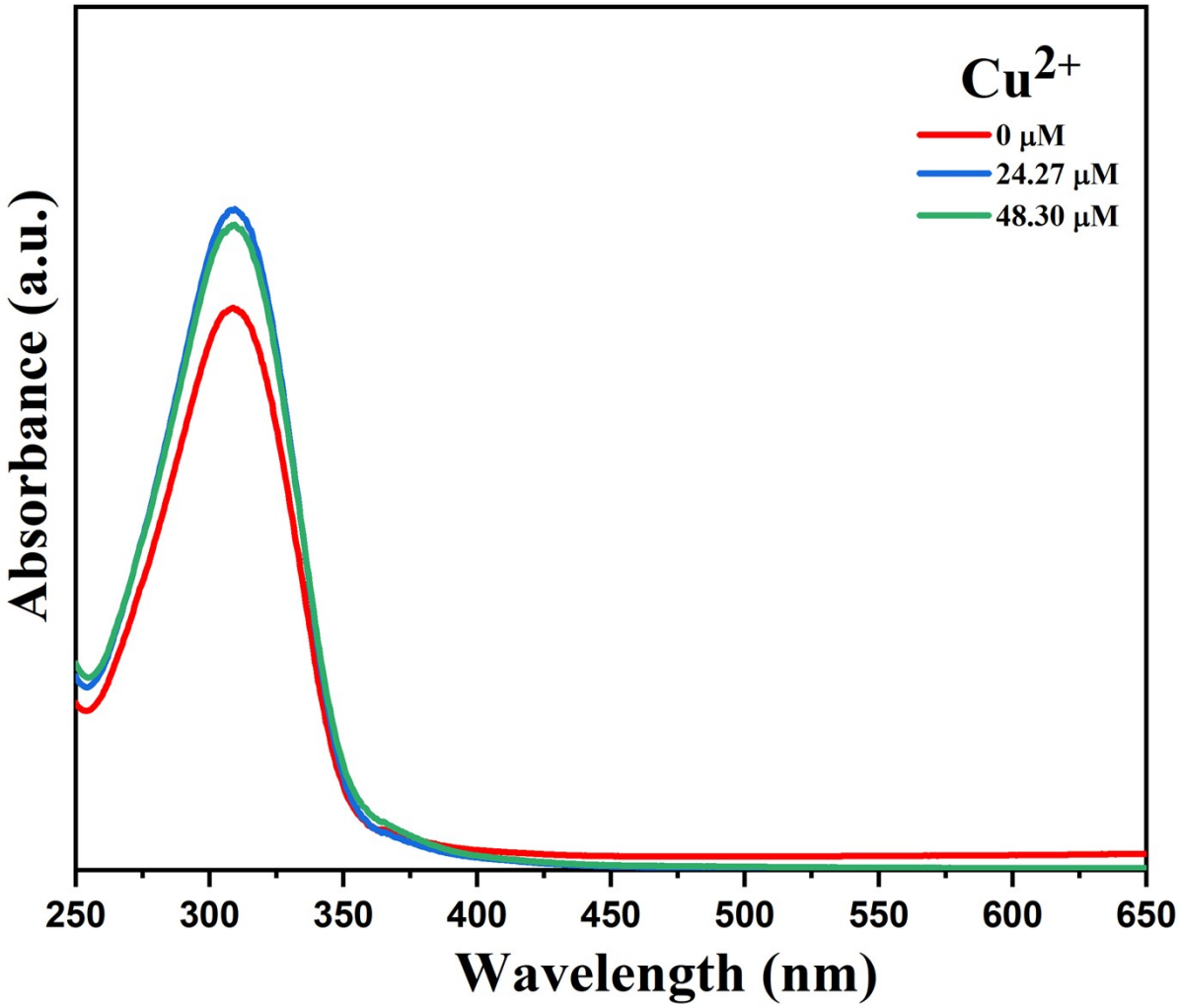

Fig. S44: Absorption spectra of **1** dispersed in water upon incremental addition of water solution of Cu^{2+} ions. Final concentration of Cu^{2+} ions in the medium is indicated in the legend.

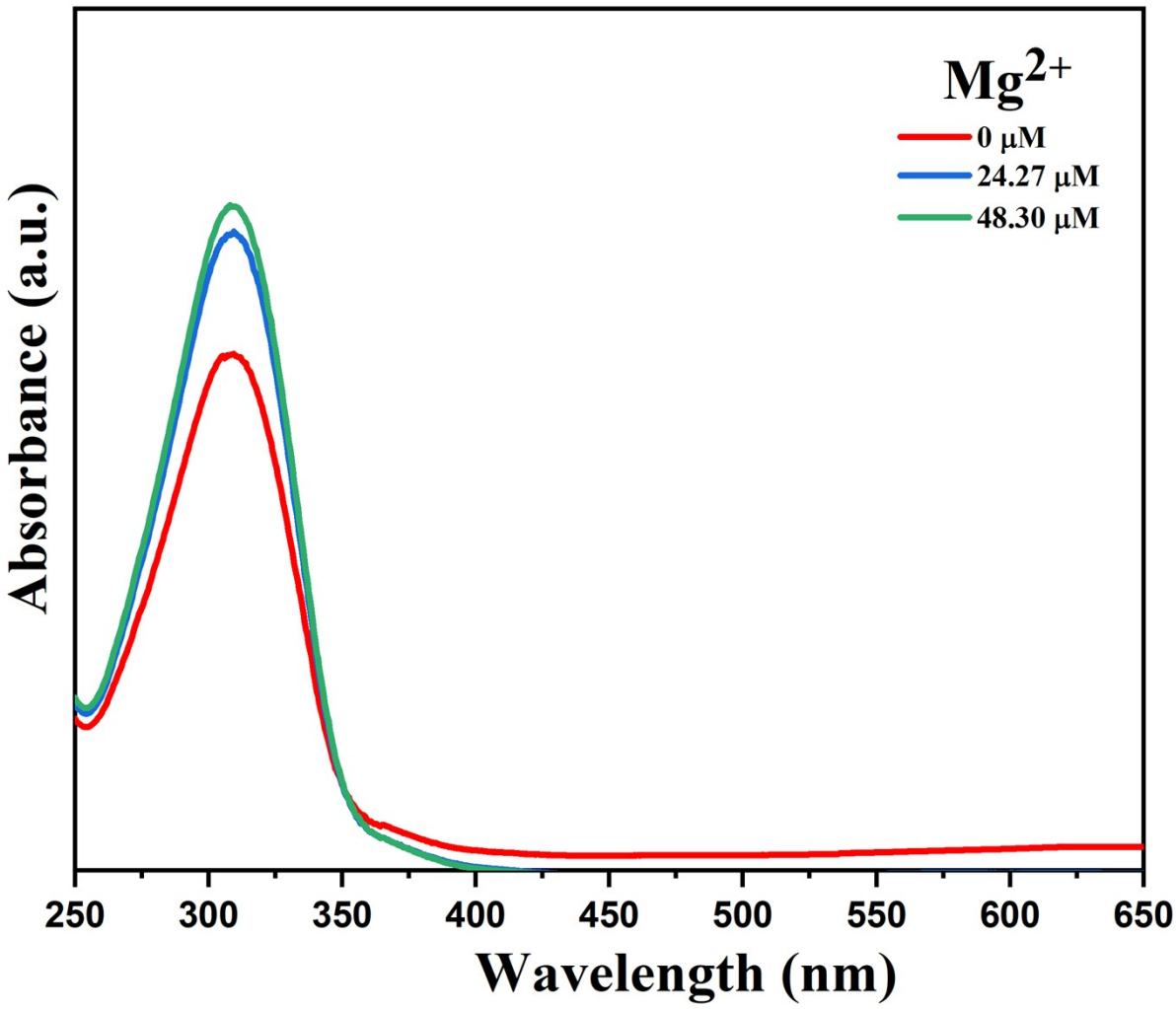

Fig. S45: Absorption spectra of **1** dispersed in water upon incremental addition of water solution of Mg^{2+} ions. Final concentration of Mg^{2+} ions in the medium is indicated in the legend.

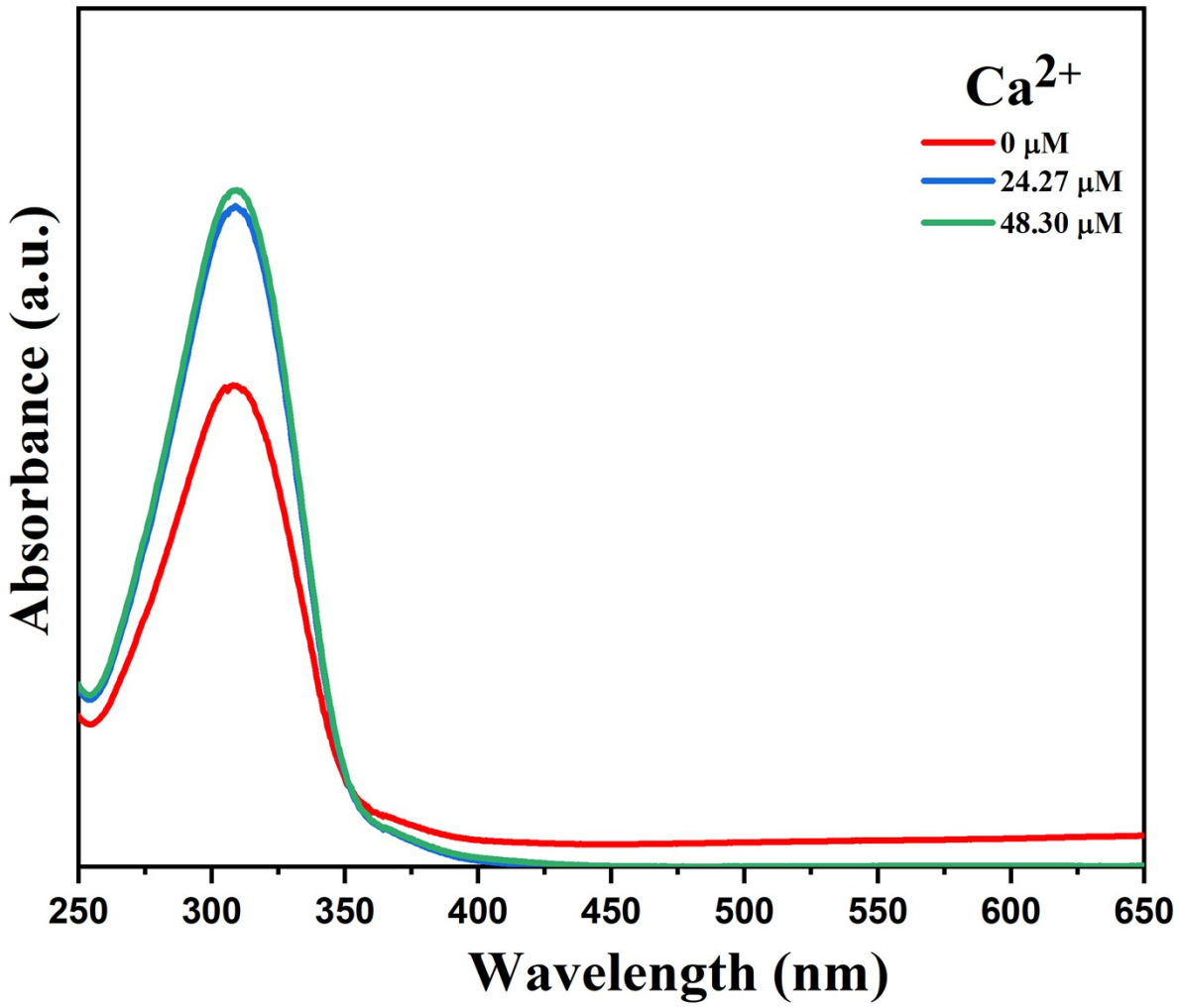

Fig. S46: Absorption spectra of **1** dispersed in water upon incremental addition of water solution of Ca^{2+} ions. Final concentration of Ca^{2+} ions in the medium is indicated in the legend.

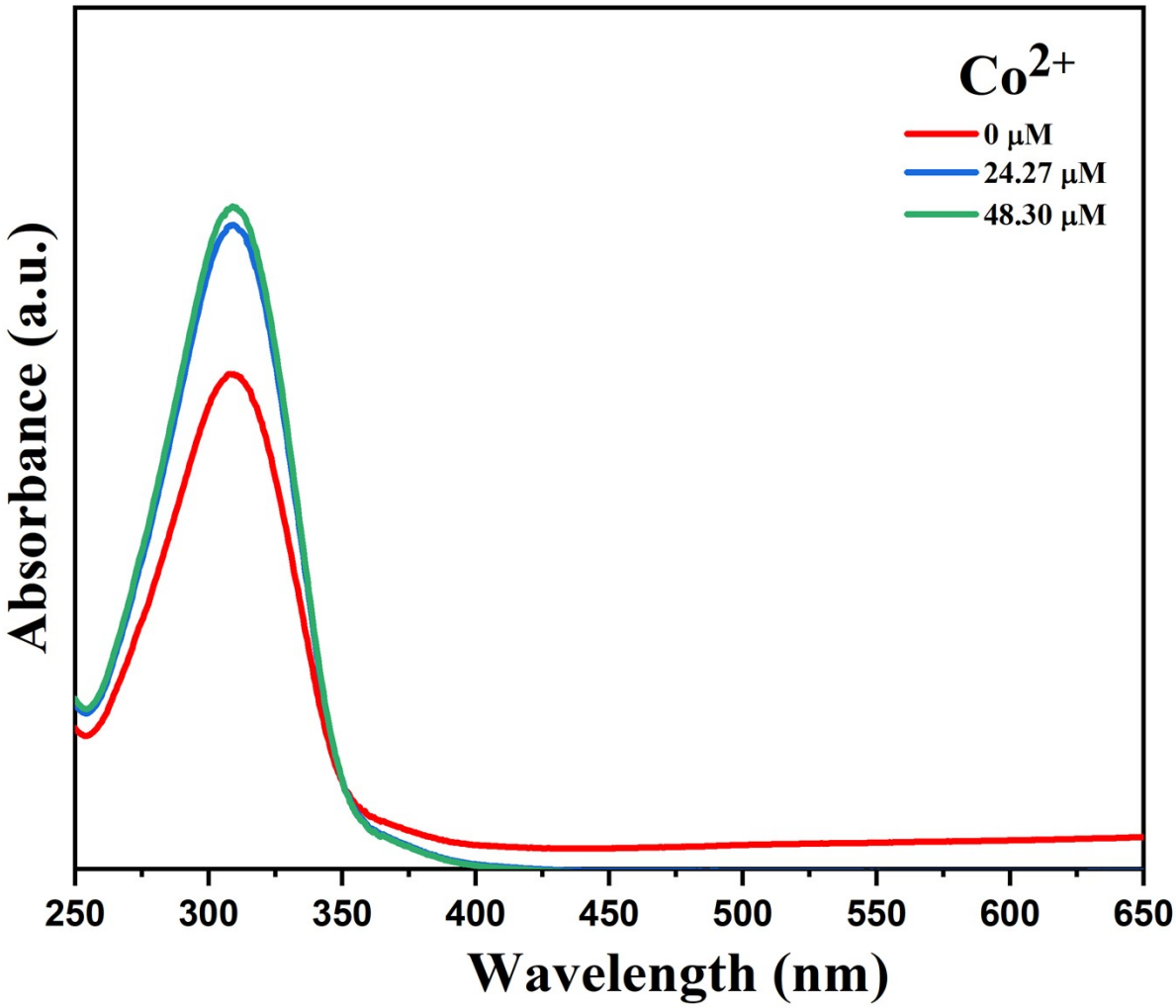

Fig. S47: Absorption spectra of **1** dispersed in water upon incremental addition of water solution of Co^{2+} ions. Final concentration of Co^{2+} ions in the medium is indicated in the legend.

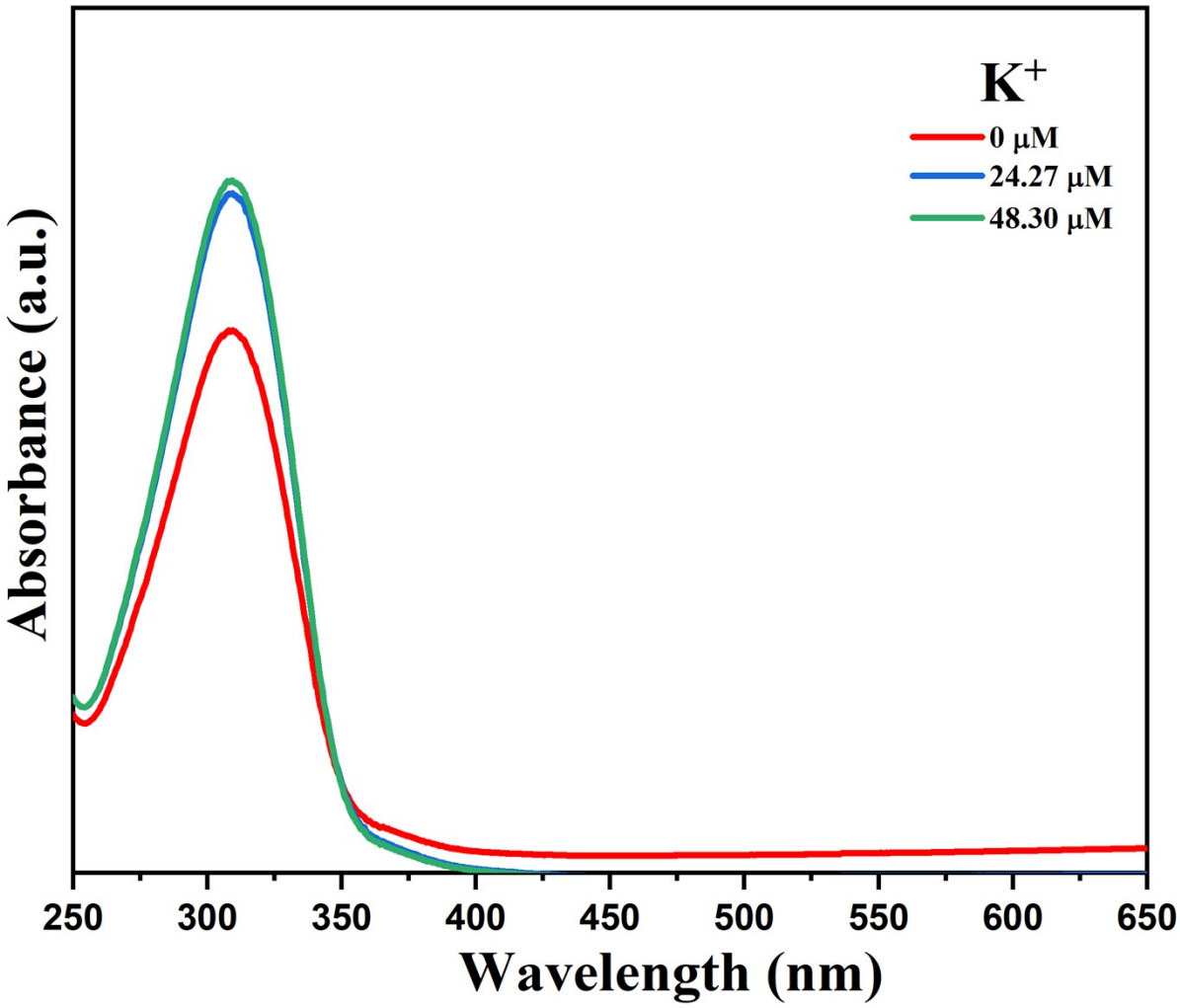

Fig. S48: Absorption spectra of **1** dispersed in water upon incremental addition of water solution of K^+ ions. Final concentration of K^+ ions in the medium is indicated in the legend.

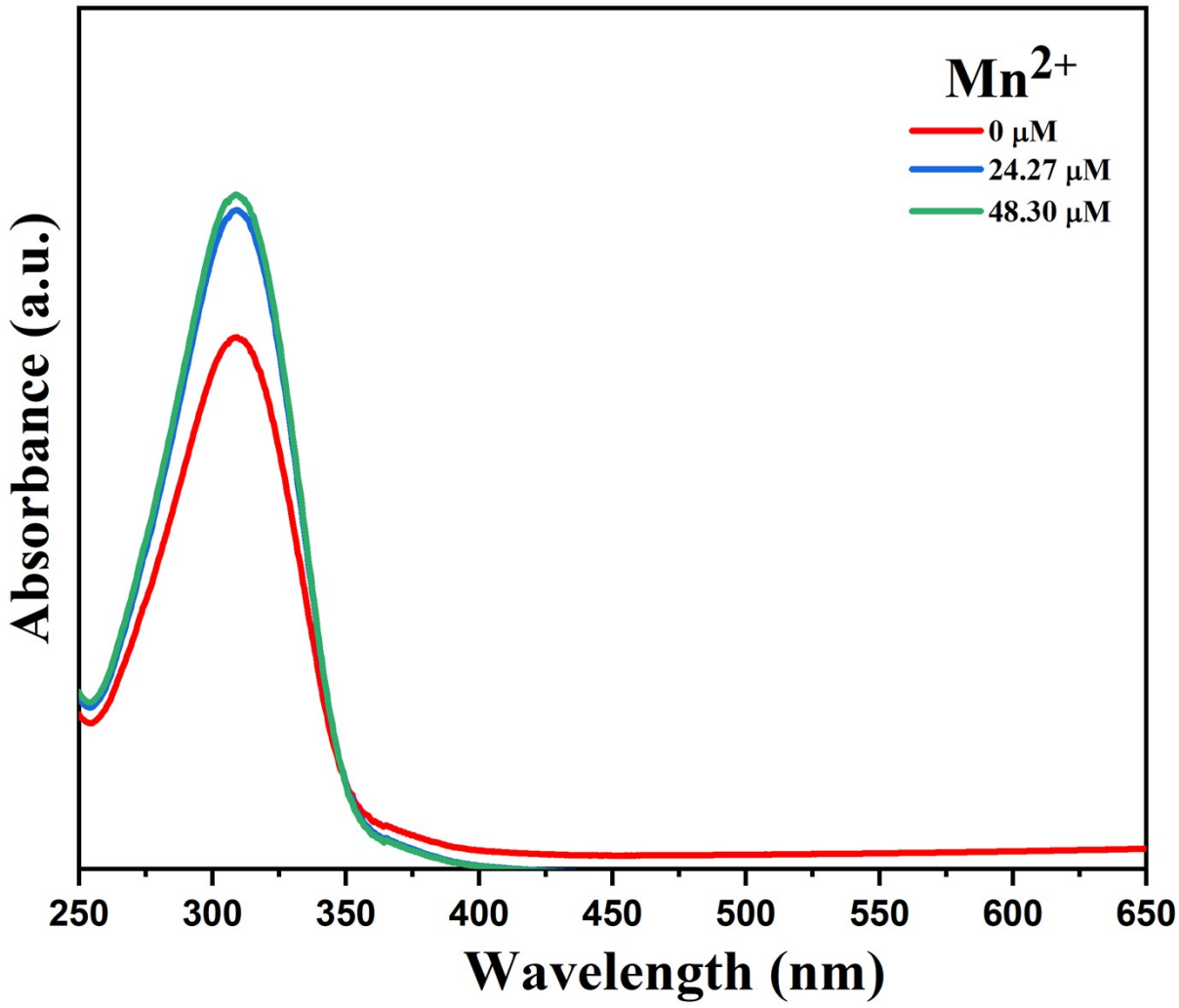

Fig. S49: Absorption spectra of **1** dispersed in water upon incremental addition of water solution of Mn^{2+} ions. Final concentration of Mn^{2+} ions in the medium is indicated in the legend.

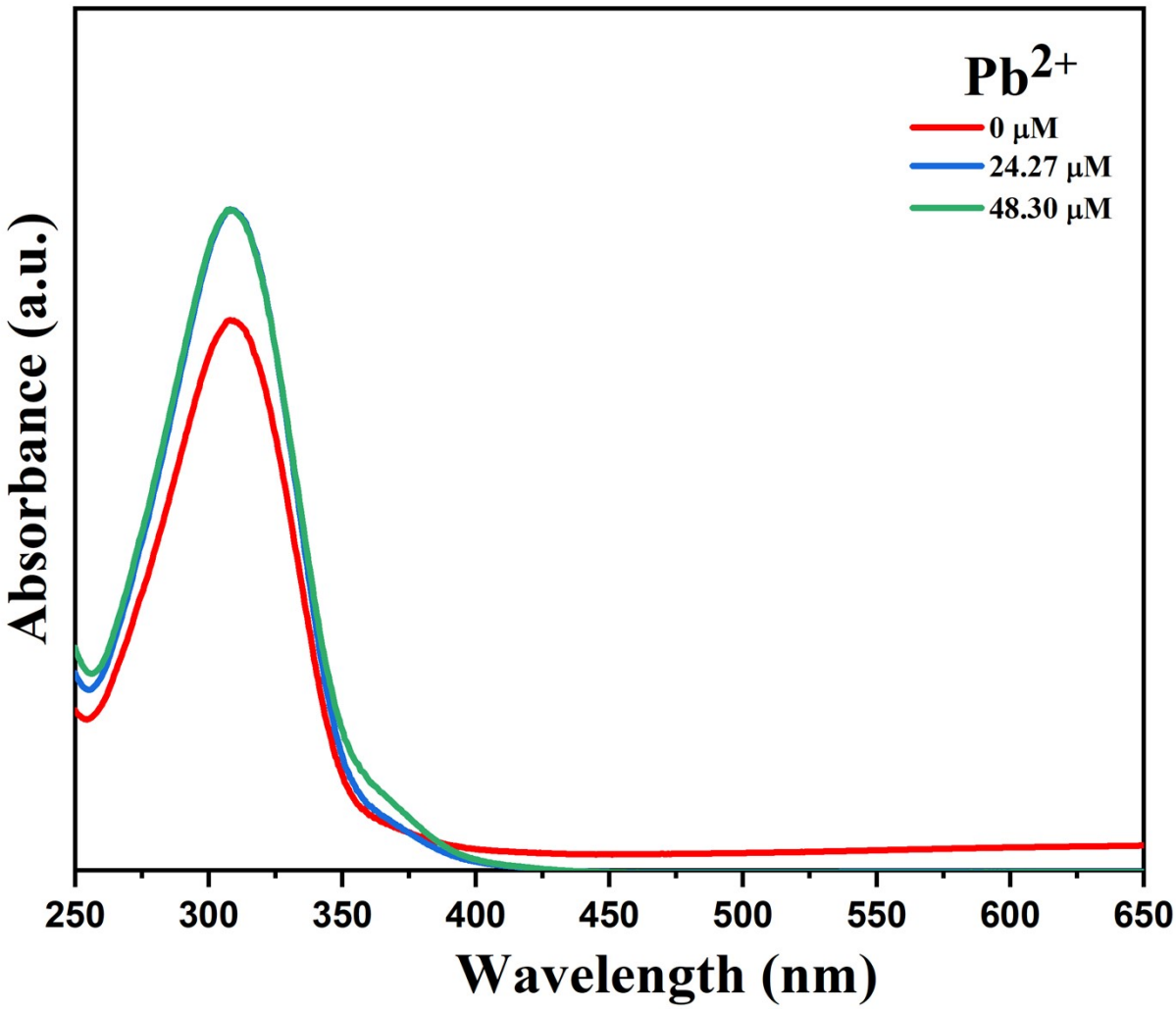

Fig. S50: Absorption spectra of **1** dispersed in water upon incremental addition of water solution of Pb^{2+} ions. Final concentration of Pb^{2+} ions in the medium is indicated in the legend.

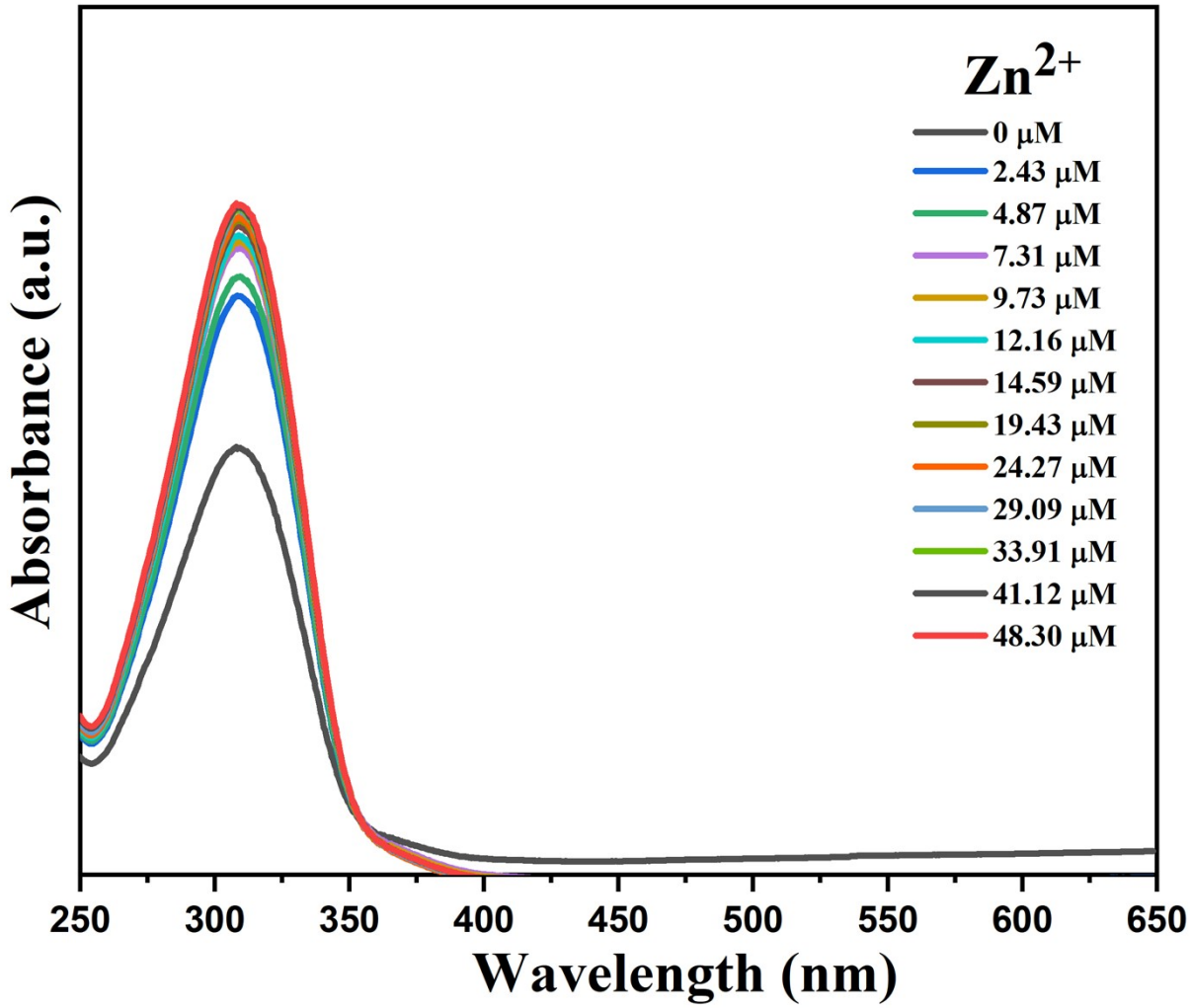

Fig. S51: Absorption spectra of **1** dispersed in water upon incremental addition of water solution of Zn^{2+} ions. Final concentration of Zn^{2+} ions in the medium is indicated in the legend.

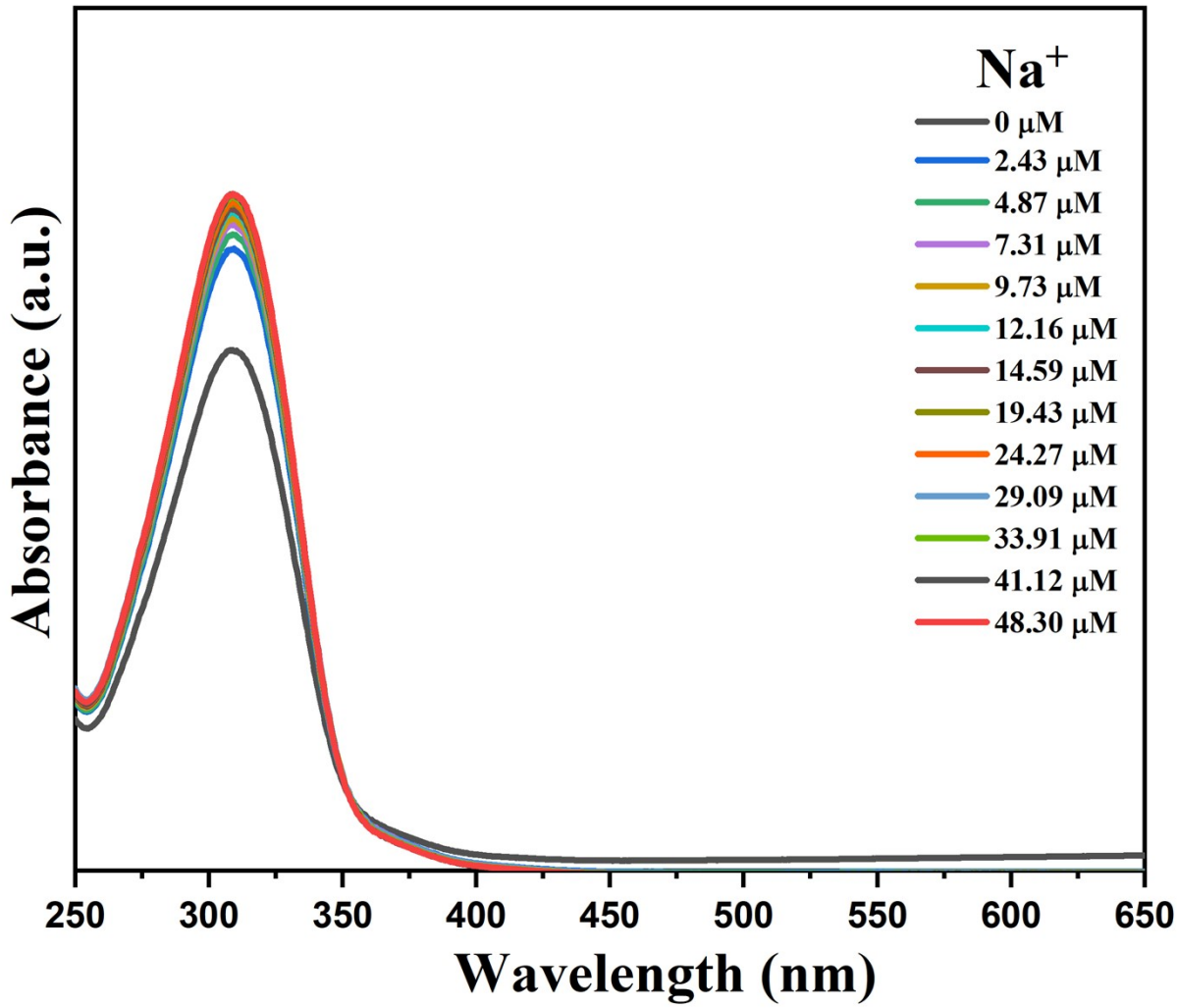

Fig. S52: Absorption spectra of **1** dispersed in water upon incremental addition of water solution of Na^+ ions. Final concentration of Na^+ ions in the medium is indicated in the legend.

Table S6: A summary of luminescence-based sensing of Fe^{3+} ion using MOFs.

MOF	Medium	LOD (μM)	K_{sv} (M^{-1})	Ref.
$\{[Cd_2(SA)_2(L)_2]\cdot H_2O\}_n$	DMF	2.4	2.1×10^4	89
$[Cd_2(OBA)_2(BPTP)(H_2O)]$	DMF	0.36	—	90
$[Zn(5\text{-}AIP)(Ald\text{-}4)]\cdot H_2O$	H_2O	0.30	9.00×10^4	91.
$[Zn(L)(bpdc)]\cdot 1.6H_2O$	DMF	5.62	1.73×10^4	92
$[Cd(H_2BDDA)]_n$	H_2O	—	8.79×10^4	93
$[Cd(PAM)(4\text{-}bpdb)_{1.5}]\cdot DMF$	H_2O	0.3	3.5×10^4	94
$[Cu(tpp)\cdot H_2O]_{2n}$	H_2O	10	4.6×10^4	95
$\{[Cd_3(L^{2-})_3(H_2O)]\cdot(DMF)\cdot(H_2O)\}_n$	DMF	—	2.07×10^4	96
$[Zn_2(oba)_2(bpy)]$	MeOH	0.3	5.8×10^4	97
Ag-MOFs(1−3)	H_2O	11.46, 15.83, 15.44	(0.936, 1.033, and 0.888) × 10^4	98
JXUST-18	EtOH	0.196	—	99
$[Cd(PDA)(L)_2]$	H_2O	1.34	23.29×10^4	This work

Table S7: A summary of luminescence-based sensing of Cr^{3+} ions using MOFs.

MOF	Medium	LOD (μM)	K_{sv} (M^{-1})	Ref.
$[Zn\ (tbda)]_n$	H_2O	180	2.68×10^3	100
$[Eu_2(tpbpc)_4 \cdot CO_3 \cdot 4H_2O] \cdot DMF \cdot solvent$	H_2O	68.8	5.14×10^2	101
$\{[Zn(H_2dhbdc)(bpycz)] \cdot 0.5H_2O\}_n$	H_2O	8.22	4.85×10^3	102
$[Zn(Br\text{-}1,4\text{-}bdc)\ (bpycz)]_n$	H_2O	4.73	4.04×10^3	102
$\{[Zn(tta)_{0.5}(m\text{-}bimb)] \cdot H_2O\}_n$	DMF	—	0.65	103
$[Zn_2(TPOM)(NH_2\text{–}BDC)_2] \cdot 4H_2O$	DMF	4.9	—	52
$[Zn(L)(H_2O)] \cdot H_2O$	H_2O	2.44	2.03×10^4	104
[Zn(5-AIP)(Ald-4)]·H2O	H_2O	0.46	2.30×10^4	91
$\{[Zn(BIBT)(oba)] \cdot DMA\}_n$	EtOH	0.049	—	105
$[Me_2NH_2]_4[Zn_6(qptc)_3(trz)_4] \cdot 6H_2O$	H_2O	1	4.39×10^4	106
$Zn_3(bpdc)_2(pdc)(DMF) \cdot 6DMF$	DMF	25.1	3870	107
$[Cd(PDA)(L)_2]$	H_2O	4.95	5.06×10^4	This work

Table S8: A summary of luminescence-based sensing of Al^{3+} ions using MOFs.

MOF	Medium	LOD (μM)	Ksv (M^{-1})	Ref.
{[Zn_2(O-BTC)(4,4′-BPY)$_{0.5}$(H_2O)$_3$]·(H_2O)$_{1.5}$·(DMA)$_{0.5}$}$_n$	EtOH	3.70	—	59
[Zn(DMA)(TBA)]	H_2O	1.97	1.33×10^4	108
[Co_2(dmimpym)(nda)$_2$]$_n$	DMF	0.7	—	109
{[Cd(CDC)(L)]}$_n$	DMF	61	2.6×10^3	89
[Cd(L)(phen)$_2$]·5H_2O	DMF	0.113	2.49×10^4	110
HPU-24@Ru	H_2O	11.63	—	111
{[Co(L)(bibp)]}$_n$	H_2O	1.52	1.97×10^4	112
[Zn(5-AIP)(Ald-4)]·H_2O	H_2O	0.35	2.80×10^4	91
[Cd(PAM)(4-bpdb)$_{1.5}$]·DMF	H_2O	0.56	2.3×10^4	113
{[Cd_2(SA)$_2$(L)$_2$]·H_2O}$_n$	DMF	93	5.4×10^3	89
[Co(OBA)(DATZ)$_{0.5}$(H_2O)]	H_2O	2.5	—	114
[Cd(PDA)(L)$_2$]	H_2O	3.96	3.09×10^4	This work

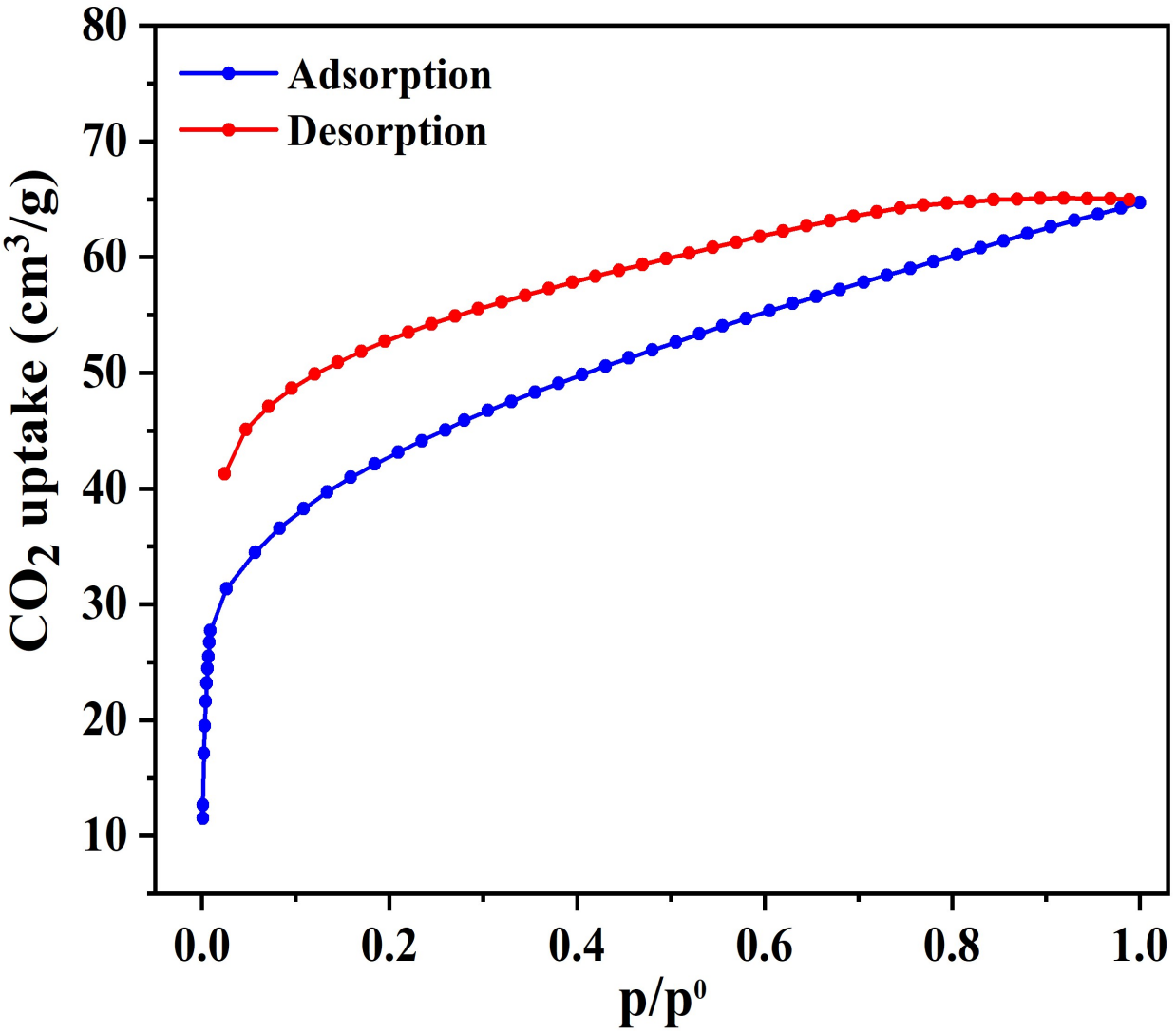

Fig. S53: CO_2 gas sorption isotherm of **1** at 195 K.

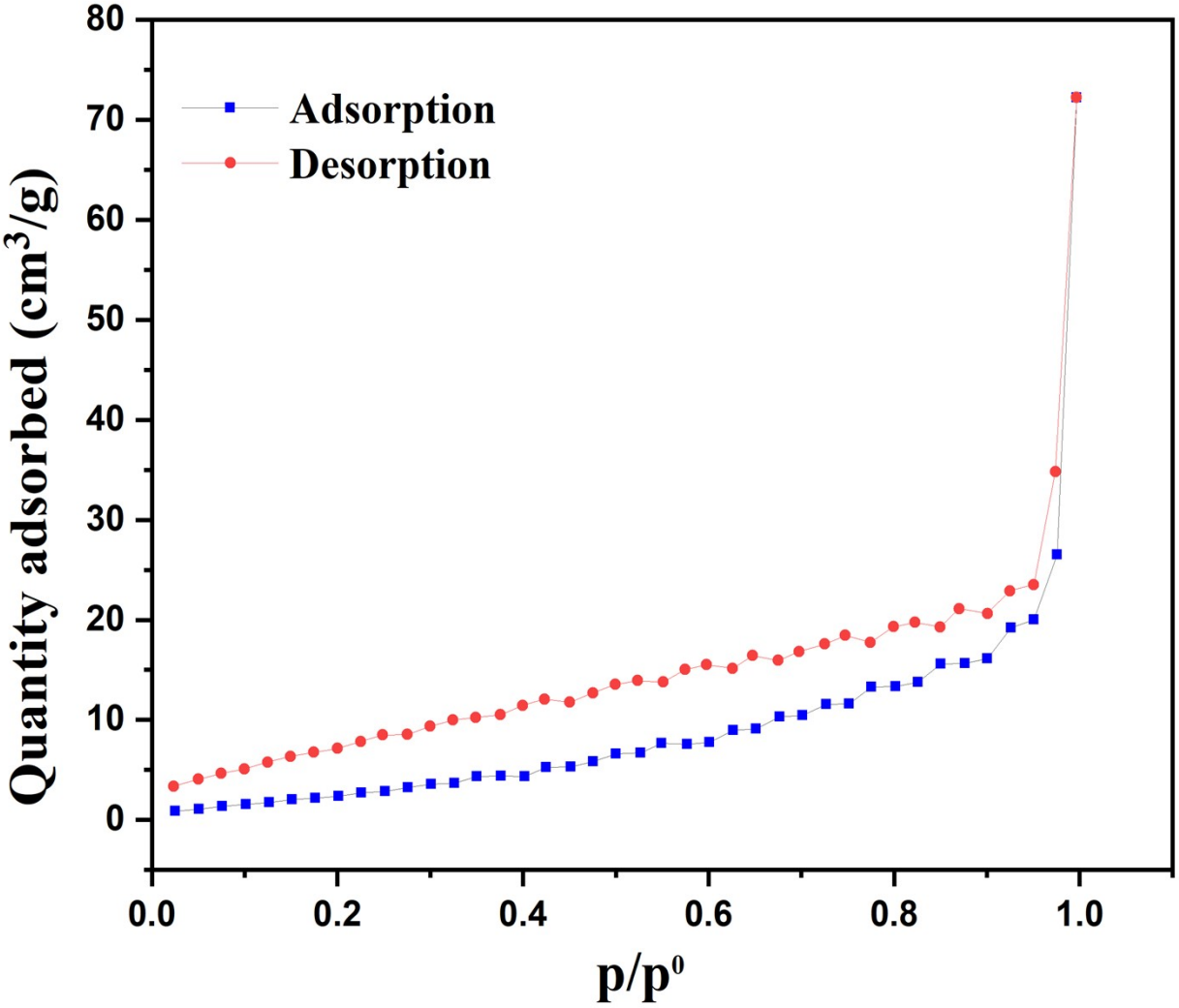

Fig. S54: N_2 gas sorption isotherm of **1** at 77 K.

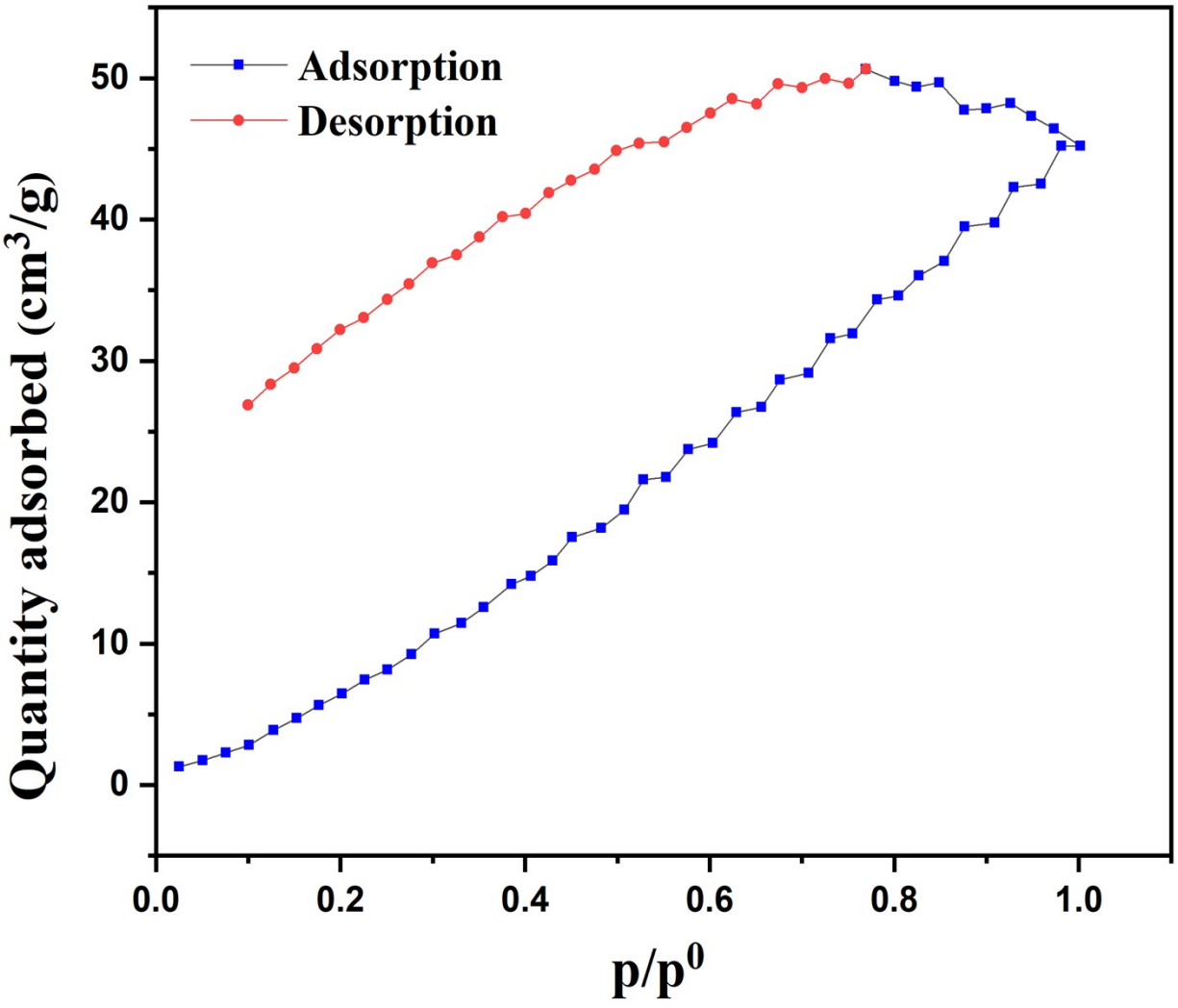

Fig. S55: H_2 gas sorption isotherm of **1** at 77 K.

Table S9: A summary of CO_2 gas adsorption using MOFs.

MOFs	Surface area from N_2 adsorption [$m^2 g^{-1}$]	CO_2 uptake cm^3/g at 195 K	Ref.
$\{[Cd_2(sdb)_2(4\text{-bpmh})_2(H_2O)]\}_n \cdot 2n(H_2O)$	—	39.19	115
$\{[Cd_2(sdb)_2(3\text{-bpmh})_2]\}_n \cdot 3n(H_2O) \cdot n(C_6H_5NO)$	—	60.9	115
$[Mg_{16}(PTCA)_8(\mu_2\text{-}H_2O)_8(H_2O)_{16}(dioxane)_8].(H_2O)_{13}.(DMF)_{26}$	438.1	160.5	116
$\{[Zn(H_2dhbdc)(bpycz)] \cdot 0.5H_2O\}_n$	291.4	101.1	102
$[Zn(Br\text{-}1,4\text{-}bdc)(bpycz)]_n$	288.5	98.6	102
Cu-MOF	945	201.6	117
$[Cu_3(3,3'\text{-}dmglut)_3(bte)] \cdot 6(H_2O)\}_n$ and $[Cu(3,3'\text{-}dmglut)(btp)_{0.5}] \cdot 2(H_2O)\}_n$	—	21 and 26.2	118
Cu–MOP	270.9	96.5	119
ZnDatzBdc	303	92.5	120
$[Cd(PDA)(L)_2]$	11.635	64.5	This work